Integrable modification of the critical Chalker-Coddington network model

Yacine Ikhlef, Paul Fendley, and John Cardy

Phys. Rev. B **84**, 144201 — Published 3 October 2011

DOI: 10.1103/PhysRevB.84.144201

An integrable modification of the critical Chalker-Coddington network model

Yacine Ikhlef
Section Mathématiques, Université de Genève
2-4 rue du Lièvre, CP 64, 1211 Genève 4, Switzerland

Paul Fendley
Microsoft Research, Station Q, University of California
Santa Barbara, CA 93106 and
Department of Physics, University of Virginia
Charlottesville, VA 22904-4714, USA

John Cardy
Rudolf Peierls Centre for Theoretical Physics, University of Oxford
1 Keble Road, OX1 3NP, United Kingdom and
All Souls College, Oxford
(Dated: September 2, 2011)

We consider the Chalker-Coddington network model for the Integer Quantum Hall Effect, and examine the possibility of solving it exactly. In the supersymmetric path integral framework, we introduce a truncation procedure, leading to a series of well-defined two-dimensional loop models, with two loop flavours. In the phase diagram of the first-order truncated model, we identify four integrable branches related to the dilute Birman-Wenzl-Murakami braid-monoid algebra, and parameterised by the loop fugacity n. In the continuum limit, two of these branches (1,2) are described by a pair of decoupled copies of a Coulomb-Gas theory, whereas the other two branches (3,4) couple the two loop flavours, and relate to an $\mathrm{SU}(2)_r \times \mathrm{SU}(2)_r/\mathrm{SU}(2)_{2r}$ Wess-Zumino-Witten (WZW) coset model for the particular values $n = -2\cos[\pi/(r+2)]$ where r is a positive integer. The truncated Chalker-Coddington model is the $n = 0$ point of branch 4. By numerical diagonalisation, we find that its universality class is neither an analytic continuation of the WZW coset, nor the universality class of the original Chalker-Coddington model. It constitutes rather an integrable, critical approximation to the latter.

PACS numbers: 73.43.Nq, 73.20.Fz, 02.30.Ik, 11.25.Hf
Keywords: Quantum Hall Effect, Plateau Transition, Integrable Models, Conformal Field Theory

I. INTRODUCTION

The transition between plateaux in the Integer Quantum Hall Effect (IQHE) is a quantum critical phenomenon, which was predicted theoretically[1,2] and observed experimentally[3] a few decades ago. Although experimentally there is no a priori reason to neglect electron-electron interactions, it is usually modelled theoretically by noninteracting particles in two dimensions (2d), in a perpendicular magnetic field and a random potential. Despite the apparent simplicity of this conceptual setup, it turns out to be very difficult to derive analytically the critical exponents of this transition. Important progress was achieved by the introduction of a simple network model which retains the salient features of guiding centre motion and quantum tunnelling in the presence of disorder: the Chalker-Coddington (CC) model[4]. Extensive numerical studies based on the CC model or other approaches have led to good estimates for the critical exponents, notably the correlation-length exponent $\nu = 2.37 \pm 0.02$[6] (a larger value $\nu = 2.593 \pm 0.006$ has also been reported[7]). Also, a semi-classical argument[8] yields the prediction $\nu = 7/3$.

The CC model is also the starting point for several analytical approaches, like the description by a σ-model[9], or a mapping to a one-dimensional (1d) quantum many-body system[10,11], and also an Algebraic Bethe Ansatz construction[12]. However, from the point of view of critical lattice models, no exact solution of the CC model has been found so far.

The situation is very different for the *spin* Quantum Hall Effect (SQHE): the generalisation of the CC model to SQHE[13] (which we shall call Sp(2)-CC) maps exactly to classical bond percolation, where a large class of exponents are known[14]. This mapping of Sp(2)-CC to classical percolation was first observed by Gruzberg *et al.*[15], who used a supersymmetric (SUSY) spin-chain formulation. Later on, it was realised[16,17] that the SUSY *lattice path integral* maps Sp(2)-CC to a statistical model of lattice paths, which are exactly the hulls of bond-percolation clusters. Moreover, a number of SQHE physical observables are expressed in terms of percolation correlation functions, and this mapping is valid even at the level of lattice models.

In this paper, we propose a treatment of the original CC model based on the lattice path integral. Since the corresponding statistical model involves paths which may pass through a given edge infinitely many times, the number of configurations per unit surface is infinite, and the model is not directly tractable by exact-solution methods such as Yang-Baxter integrability and Conformal Field Theory (CFT). We therefore introduce a *truncation procedure*, leading to a series of finite statistical models, and focus on the first order of truncation. The arising model is a two-colour loop model including vacancies, and with loop fugacity $n = 0$.

Integrable multi-colour loop models have been known for a long time[18]. They were originally defined through multi-dimensional height models, but they may as well describe coupled copies of classical magnetism models, such as the Potts or O(n) models, and also the ground state of *quantum* loop models. More specifically, in a two-colour, completely packed (*i.e.* without vacancies) loop model[19,20], new integrable points were identified through a mapping to a braid-monoid algebra: the Birman-Wenzl-Murakami (BWM) algebra[21] (see also[22] for integrable two-colour loop models related to two coupled Potts models). In the present paper, we use a similar approach on the loop model arising from our truncation procedure, which is a two-colour loop model including vacancies. Generalising to arbitrary loop fugacity n, we obtain four critical branches in the phase diagram of this loop model. We then study the critical properties of these branches.

We find that two of these regimes (denoted 1 and 2) correspond to a pair of decoupled Coulomb-Gas (CG) theories, whereas the other two (3 and 4) relate to the $\mathrm{SU}(2)_r \times \mathrm{SU}(2)_r/\mathrm{SU}(2)_{2r}$ Wess-Zumino-Witten coset model, for values $n = \pm 2\cos\frac{\pi}{r+2}$ with $r \in \{1, 2, 3, \dots\}$. We obtain analytically two critical exponents: one of them, X_{int}, corresponds to an elliptic deformation of the integrable weights, and the other one, $X_{(1,1;\mathrm{adj})}$, is associated to a perturbation of the weight per monomer. The truncated, modified CC model is realised by the $n = 0$ point of regime 4, but this point is outside the validity range for the analytic continuation of the WZW exponents. Our numerical study gives the estimate $\nu \simeq 1.1$ for the correlation-length exponent, and $d_f \simeq 1.71$ for the fractal dimension of paths. This is clearly incompatible with the IQHE universality class, and hence our integrable two-colour loop model is only a crude approximation to IQHE. However, the truncation procedure may be carried out to higher orders, possibly yielding more accurate, solvable approximations.

The plan of the paper is as follows. In Section 2, we recall the definition of the CC model and its lattice SUSY path-integral formulation, and explain our truncation procedure,resulting in a two-colour loop model. This truncation is compared in detail with the one used in[10,11]. In Section 3, we use a mapping to a dilute braid-monoid algebra to derive the integrable Boltzmann weights of the two-colour loop model, as well as the corresponding 1d Hamiltonian. In Section 4, we identify the four critical regimes of the integrable model and the corresponding CFTs. Numerical and analytical support for the identification of these CFTs is given. In Section 5, we examine in more detail regime 4, which contains the truncated, modified CC model at $n = 0$. We discuss the analytic continuation of CFT results, and estimate numerically some critical exponents, including the correlation-length exponent ν.

The paper has three appendices. Appendix A contains the details of the mapping to the dilute BWM (dBWM) algebra used in Section 3. In Appendix B, we exhibit a lattice holomorphic parafermion $\psi_s(z)$ in the integrable model.

In Appendix C, we expose the exact solution of a particular point in regime 4, which is mapped to free fermions. This mapping provides a valuable check on our results, and also gives a proof that the O($n = 1$) loop model has central charge $c = \frac{1}{2}$.

II. TRUNCATION OF THE CHALKER-CODDINGTON MODEL

A. The Chalker-Coddington model

The Chalker-Coddington model[4] is a simple lattice model for the IQHE. The latter consists of a two-dimensional gas of non-interacting electrons in a disordered medium, subject to a strong transverse magnetic field. In the presence of the random potential, the Landau levels are broadened, and eigenenergies are of the form $E = \left(k + \frac{1}{2}\right)\hbar\omega_c + V_0$, where k is an integer, ω_c is the cyclotron energy of the electron in the magnetic field, and V_0 is a random part. Let us recall briefly the main ingredients of the CC model.

We consider an electron in the eigenstate of energy E. The spatial trajectories of the electron over finite time steps Δt are modelled by paths on the directed square lattice $\mathcal{L}$ (see Fig. 1), and the time-evolution operator over Δt is denoted $\mathcal{U}$. The operator $\mathcal{U}$ reads

$$\mathcal{U} = \bigotimes_{\text{edge } e} U_e \bigotimes_{\text{vertex } v} U_v \,, \tag{1}$$

with two types of factors:

- On each directed edge e, the operator U_e takes the particle along e and multiplies the wavefunction by a random Aharonov-Bohm phase $\exp(i\phi_e)$, where the ϕ_e are independent and uniformly distributed on the interval $[0, 2\pi]$.
- At each vertex v, the operator U_v scatters the particle to one of the outgoing edges. In the bases $(1, 2)$ and $(3, 4)$ of Fig. 1, U_v is represented by the unitary matrix:

$$S = \begin{pmatrix} \tanh\beta & 1/\cosh\beta \\ 1/\cosh\beta & -\tanh\beta \end{pmatrix} . \tag{2}$$

The parameter β measures the distance to the plateau transition at $E = E_c = \left(k + \frac{1}{2}\right)\hbar\omega_c$. The critical value is $\beta_c = \log(1 + \sqrt{2})$, and the corresponding energy perturbation is assumed to behave as[4]

$$(E - E_c) \propto (\beta - \beta_c) \,. \tag{3}$$

No exact solution of the CC model is known, in the sense that the critical exponents have not been determined analytically. However, very good numerical estimates exist for some of these exponents[5–7]. In particular, the correlation-length exponent $\nu_{\rm CC}$, defined by the scaling of the correlation length

$$\xi \propto |E - E_c|^{-\nu_{\rm CC}} \,, \tag{4}$$

has been estimated as[6]

$$\nu_{\rm CC} \simeq 2.37 \pm 0.02 \,. \tag{5}$$

B. Path integral representation

The problem of solving the CC model amounts to the diagonalisation of a random time-evolution operator. We want to perform the average over disorder, in order to turn this into a translationally invariant 2d classical model. For this purpose, we use the supersymmetric path integral representation[23]. The following derivation is very analogous to what was done by one of us for the SQHE[17], and we use the notations of[17] throughout this Section.

The Green's function between two edges e_1 and e_2 is:

$$G(e_2, e_1, z) := \langle e_2|(1 - z\mathcal{U})^{-1}|e_1\rangle \,. \tag{6}$$

Here z is a parameter which plays the role of the energy in the usual Green's function $(E - \mathcal{H})^{-1}$: roughly speaking $z \sim e^{iE}$, where E is measured from the filled Landau level. We label e_L, e_R the ends of any edge e, with the convention

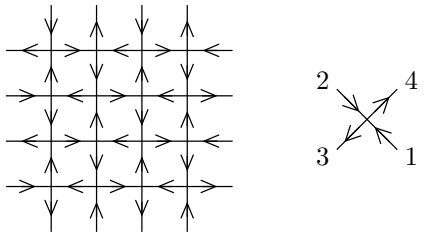

(a) (b)

FIG. 1. (a) Oriented square lattice $\mathcal{L}$ for the Chalker-Coddington model. (b) Labelling of the edges adjacent to a vertex of $\mathcal{L}$.

that it is directed in the sense $e_R \to e_L$, and we introduce the complex variables $b_L(e), b_R(e)$. The Gaussian measure is defined as:

$$\int [\mathrm{d}b]\ (\dots) := \frac{1}{\pi} \int \mathrm{d}(\mathrm{Re}\ b)\ \mathrm{d}(\mathrm{Im}\ b)\ \ \exp(-b^* b)(\dots)\,, \qquad [\mathrm{D}b] := \prod_e [\mathrm{d}b_L(e)][\mathrm{d}b_R(e)]\,. \tag{7}$$

The Green's function can then be written as a Gaussian integral on the $b_L(e), b_R(e)$:

$$G(e_2, e_1, z) = \frac{\int [\mathrm{D}b]\ b_L(e_2) b_L^*(e_1) \exp A_b}{\int [\mathrm{D}b]\ \exp A_b}\,, \tag{8}$$

where the action reads

$$A_b = A_b^{(\mathrm{edge})} + A_b^{(\mathrm{vertex})}\,, \tag{9}$$

$$A_b^{(\mathrm{edge})} = z \sum_{\mathrm{edge}\ e} b_L^*(e) \exp(i\phi_e) b_R(e)\,, \tag{10}$$

$$A_b^{(\mathrm{vertex})} = \sum_{\mathrm{vertex}\ v} \sum_{i \underset{v}{\to} j} b_R^*(e_i) S_{ij} b_L(e_j)\,, \tag{11}$$

and the notation $i \underset{v}{\to} j$ means that i (resp. j) is an incoming (resp. outgoing) edge adjacent to v. The next step is to express the denominator in (8) as the inverse of a Gaussian integral over Grassmann variables $f_{L,R}(e), \bar{f}_{L,R}(e)$:

$$G(e_2, e_1, z) = \int [\mathrm{D}b][\mathrm{D}f]\ b_L(e_2) b_L^*(e_1) \exp(A_b + A_f)\,, \tag{12}$$

with the measure

$$\int [\mathrm{d}f]\ (\dots) := \int \mathrm{d}\bar{f}\ \mathrm{d}f\ \ \exp(-\bar{f} f)(\dots)\,, \qquad [\mathrm{D}f] := \prod_e [\mathrm{d}f_L(e)][\mathrm{d}f_R(e)]\,, \tag{13}$$

and A_f is the analog of A_b, with b, b^* replaced by $f, \bar{f}$.

We denote by an overbar the quenched average over the variables ϕ_e. A useful formula for this computation is

$$\frac{1}{2\pi} \int_0^{2\pi} \mathrm{d}\phi \exp\left(u e^{i\phi} + v^* e^{-i\phi}\right) = \sum_{m=0}^{\infty} \frac{(uv^*)^m}{(m!)^2}\,. \tag{14}$$

It easy to see, for instance, that $\overline{G(e_2, e_1, z)} = \delta(e_1, e_2)$. When studying transport properties, the main quantity of interest is $\overline{|G|^2}$. We write

$$\begin{aligned} |G(e_2, e_1, z)|^2 &= \int [\mathrm{D}b][\mathrm{D}f]\ b_L(e_2) b_L^*(e_1)\ e^{A_b + A_f} \times \int [\mathrm{D}b][\mathrm{D}f]\ b_L^*(e_2) b_L(e_1)\ e^{A_b^* + A_f^*} \\ &= \int [\mathrm{D}b_{1,2}][\mathrm{D}f_{1,2}]\ b_{L1}(e_2) b_{L1}^*(e_1) b_{L2}^*(e_2) b_{L2}(e_1)\ e^{A_{b1} + A_{f1} + A_{b2}^* + A_{f2}^*}\,. \end{aligned} \tag{15}$$

Using (14), we get:

$$\overline{|G(e_2,e_1,z)|^2} = \int [\mathrm{D}b_{1,2}][\mathrm{D}f_{1,2}]\; b_{L1}(e_2)b^*_{L1}(e_1)b^*_{L2}(e_2)b_{L2}(e_1)\times$$
$$\exp\left[A^{(\mathrm{vertex})}_{b1} + A^{(\mathrm{vertex})*}_{b2} + A^{(\mathrm{vertex})}_{f1} + A^{(\mathrm{vertex})*}_{f2}\right]\times$$
$$\prod_e \sum_{m_e=0}^{\infty} \frac{(z^*z)^{m_e}}{(m_e!)^2}\left\{\left[b^*_{L1}(e)b_{R1}(e) + \bar{f}_{L1}(e)f_{R1}(e)\right]\left[b^*_{R2}(e)b_{L2}(e) + \bar{f}_{R2}(e)f_{L2}(e)\right]\right\}^{m_e}. \qquad (16)$$

The expression (16) for $\overline{|G|^2}$ can be interpreted graphically as follows. Each term in the expansion of the product corresponds to a pair of paths (γ_1,γ_2), where γ_1 respects the orientation of the lattice $\mathcal{L}$ (forward path) and γ_2 follows the reverse orientation (backward path). The two paths must use each edge e the same number of times m_e. Paths configurations are weighted by the elements of the vertex S-matrix, and an additional factor $(z^*z)^{m_e}$. Note that closed loops have a vanishing weight, because the bosonic and fermionic contributions cancel each other.

C. Truncation procedure

In the form (16), $\overline{|G|^2}$ can be viewed as a two-point correlation function in a classical, two-dimensional statistical model for two-colour path configurations. No approximation has been introduced so far, and thus (16) is identical to the value of $\overline{|G|^2}$ in the original CC model. The main difficulty in evaluating (16) is that the paths γ_1,γ_2 may go through a given edge an arbitrary number of times m_e, and thus the statistical model has an infinite number of degrees of freedom per edge. This type of problem is not usually tractable by exact solution methods, so we need to *truncate* the statistical model to a finite loop model in order to use these methods. This is very analogous to what Nienhuis did for the O(n) spin model[24] on the hexagonal lattice: in that context, the spin model with variables ($\mathbf{S}_j \in \mathbb{R}^n, \mathbf{S}_j^2 = 1$) was formally mapped to a polygon model where edges could be used an arbitrary number of times, but the substitution $e^{J\mathbf{S}_i\cdot\mathbf{S}_j} \to 1 + J\mathbf{S}_i\cdot\mathbf{S}_j$ in the edge interaction led to a finite loop model, while preserving the O(n) symmetry of the original spin model.

The truncation we propose consists in keeping only the terms of (16) with $m_e \in \{0,1\}$, *i.e.* the configurations where each of the paths γ_1,γ_2 visits an edge at most once. This preserves the boson/fermion supersymmetry, ensuring that closed loops still have a vanishing weight in the truncated model. This can be seen as follows. In the original expression (10) for the action on the edges, we can imagine choosing a different fugacity z_e for each edge (so that it now appears inside the summation over e.) This does not affect the supersymmetry of the action. On expanding in powers of all the z_e, the bosonic contribution to a given edge now enters with a factor $(z^*_e z_e)^{m_e}$. Thus our truncation to $m_e \in \{0,1\}$ amounts to keeping only the terms up to first order in the expansion of the partition function in powers of $z^*_e z_e$, and then setting all the $z_e = z$ again.. Note that to this order we have either nothing, or a pair of bosons of different flavours (1 and 2), or a pair of fermions of different flavours, propagating along each edge. The supersymmetry ensures that each closed loop is counted with weight 0. At this stage it is simpler to switch to a replica formulation rather than using supersymmetry explicitly: we have a model with two flavours of boson, such that each edge is either unoccupied, or occupied by each flavour exactly once. Each closed loop is counted with a fugacity n, taking then $n = 0$. The vertices are shown in Fig. 2.

We briefly comment on how higher order truncations would look in this expansion. For example, at $\mathrm{O}\big((z^*_e z_e)^2\big)$ we would have either 2 pairs of bosons of each flavour, or 1 pair of bosons and 1 pair of fermions. (We can never have more than one pair of fermions because the Grassmann variables square to zero.) Note that in such a truncation we could give such a configuration a weight different from $(z^*_e z_e)^2$ and still preserve the supersymmetry. This points to the existence of an infinite-dimensional space of possible supersymmetric truncations. However in this paper we consider only the simplest.

We denote by $\overline{|G(e_2,e_1,z)|^2_{\mathrm{tr}}}$ the truncated analog of $\overline{|G(e_2,e_1,z)|^2}$: $\overline{|G(e_2,e_1,z)|^2_{\mathrm{tr}}}$ is given by the same expression as (16), but with the sum running only over $m_e = 0,1$. Then $\overline{|G(e_2,e_1,z)|^2_{\mathrm{tr}}}$ is interpreted as a two-point function in the loop model defined by the loop vertices of Fig. 2 and with loop weight $n = 0$.

In the original CC model, the parameter β in the S-matrix (2) is staggered. It is useful to consider an anisotropic version of this, where it takes the value β on the even sublattice of $\mathcal{L}$ and β' on the odd sublattice. In this anisotropic CC model, the critical line is[4]:

$$\sinh\beta\;\sinh\beta' = 1\,. \qquad (17)$$

The Boltzmann weights of the truncated loop model are defined in Fig. 2. For general β, β' they take the values:

$$\begin{array}{ll} t\,, u_1, u_2, w_1, w_2, x\ = 1,\ a\ ,\ b\ ,\ a^2\ ,\ b^2\ ,\ -a\,b & \text{(even sublattice)}, \\ t', u_1', u_2', w_1', w_2', x' = 1,\ b',\ a',\ b'^2,\ a'^2,\ -a'b' & \text{(odd sublattice)}, \end{array} \tag{18}$$

where

$$\begin{array}{ll} a\ := z^2 \cosh^{-2}\beta\ , & b\ := z^2 \tanh^2 \beta\ , \\ a' := z^2 \cosh^{-2}\beta'\,, & b' := z^2 \tanh^2 \beta'\,. \end{array} \tag{19}$$

Note that at the isotropic point these weights are

$$1,\ z^2/2,\ z^2/2,\ z^4/4,\ z^4/4,\ -z^4/4\,. \tag{20}$$

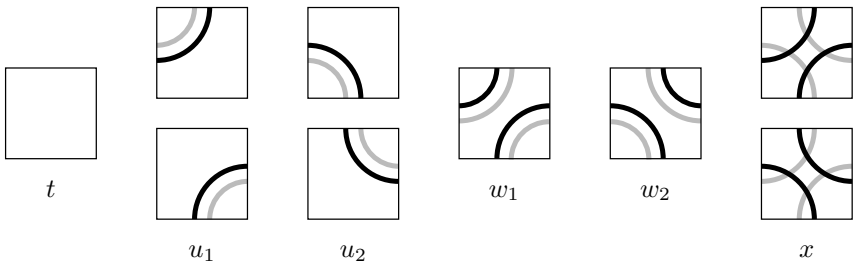

FIG. 2. Vertices of the loop model arising from the truncation of the CC model.

D. Critical properties

We now discuss the observables of the model, especially the mean square Green's function between two edges $\overline{|G(e_2, e_1, z)|^2}$. As pointed out in[25], this has to be distinguished from the point-contact conductance $P(e_2, e_1, z)$: $|G(e_2, e_1, z)|^2$ is defined for any boundary conditions, whereas the point-contact conductance refers to a set-up where one cuts open the two edges e_1 and e_2, and hence involves only the forward paths going from e_1 to e_2 without visiting e_1 or e_2 any other time (and the analogous backward paths). However, in this graphical interpretation, one clearly sees that the two quantities $|G|^2$ and P do coincide in the truncated model.

At $z = 1$ in the untruncated model, for a system without any open boundary contacts, $\overline{|G(e_2, e_1, z)|^2}$ is identically equal to one by conservation of probability. It is given by the sum over all pairs of Feynman paths going out and back from e_1 to e_2, such that each edge is traversed the same number of times in the forward path as in the return path, and weighted by the appropriate S-matrix elements of the CC model. It has been argued[26] that the weights for such 'pictures' are all positive. For $z \to 1^-$ and on the critical line (17) we expect a scaling form

$$\overline{|G(e_2, e_1, z)|^2} \sim F\left[r(1-z)^{1/d_f^{\rm CC}}\right]\,, \tag{21}$$

where $r = |e_1 - e_2|$ and $d_f^{\rm CC}$ is the fractal dimension of these pictures (whereby their total mass M behaves as r^{d_f}). The absence of the prefactor of the form $r^{-2X_{|G|^2}}$ is a consequence of the fact that $|G(z=1)|^2 = 1$ for a closed system.

In the *truncated* model, we no longer have probability conservation and so the point $z = 1$ is no longer special. Instead, in analogy with other loop models, we expect to find a different critical point, at $z = z_c$, such that the average loop length is finite for $z < z_c$ and diverges for $z \geq z_c$. The function $\overline{|G(e_2, e_1, z)|^2_{\rm tr}}$ now corresponds to the weighted sum of a pair of black and grey paths connecting e_1 and e_2. On the critical line and as $z \to z_c^-$ we expect the same scaling form as (21):

$$\overline{|G(e_2, e_1, z)|^2_{\rm tr}} \sim r^{-2X_{|G|^2}}\, F\left[r(z_c - z)^{1/d_f}\right]\,, \tag{22}$$

but not necessarily with the same dimension d_f and scaling function F as in the full model. In Figure 3 and Table I, we show the numerical determination of z_c using the two largest eigenvalues Λ_0, Λ_1 of the transfer matrix. These eigenvalues define the thermal exponent X_t through the CFT form of the free-energy gap:

$$\log \frac{\Lambda_0}{\Lambda_1} \simeq \frac{2\pi X_t}{L}\,. \tag{23}$$

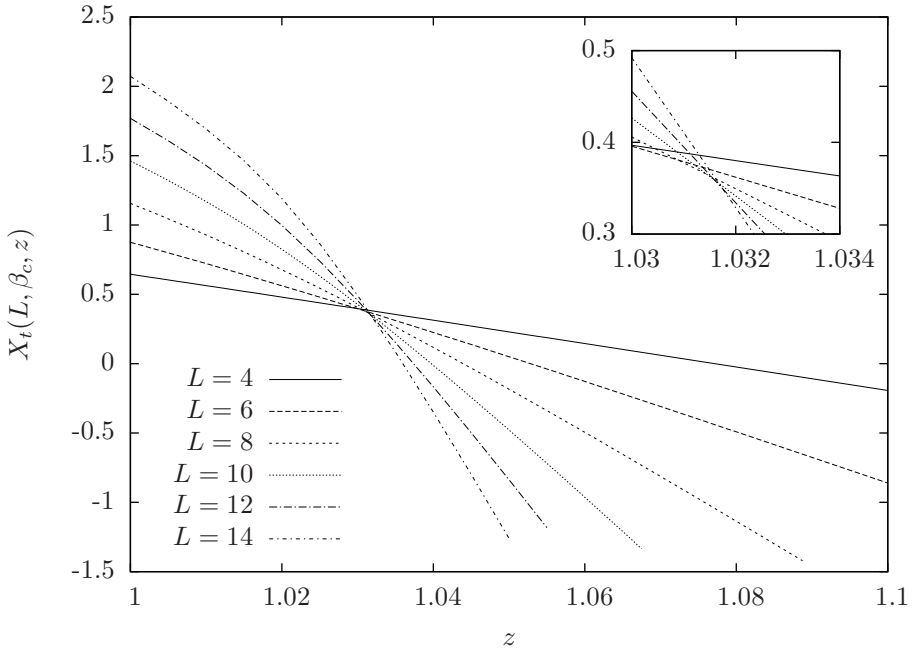

FIG. 3. Numerical determination of the critical monomer fugacity z_c in the model of Fig. 2. On the y-axis is plotted the effective thermal exponent $X_t(L, \beta_c, z) = \frac{L}{2\pi} \log \frac{\Lambda_0}{\Lambda_1}$.

L	4	6	8	10
$z_c(L, L+2)$	1.029885	1.030895	1.031454	1.031695

TABLE I. Finite-size estimates of the critical monomer fugacity z_c in the model of Fig. 2. The value $z_c(L, L+2)$ is defined as the solution of $X_t(L, \beta_c, z) = X_t(L+2, \beta_c, z)$, where $X_t(L, \beta, z) = \frac{L}{2\pi} \log \frac{\Lambda_0}{\Lambda_1}$ is the effective thermal exponent.

More generally, it is possible to consider 'watermelon' exponents X_{ℓ_1,ℓ_2} corresponding to ℓ_1 black and ℓ_2 grey paths originating from the vicinity of a given edge. The truncation constraint of course implies that these cannot originate on the same edge for $\ell > 1$, but we imagine taking the scaling limit where edges a finite distance apart on the lattice are mapped to the same point. These operators are well suited for a transfer-matrix-based numerical analysis[27].

In particular we see that $X_{1,1}$ corresponds to $X_{|G|^2}$ in (22). Also, since $z^* z$ counts the number of edges connected to two black and two grey paths, we have

$$d_f = 2 - X_{2,2}\,. \tag{24}$$

Using transfer-matrix diagonalisation, we obtain the value

$$X_{2,2} = X_t \simeq 0.3\,. \tag{25}$$

Finally, we evaluate the correlation-length exponent ν associated to a perturbation of the parameter β away from β_c. For the lowest free-energy gap we expect the scaling form

$$\log \frac{\Lambda_0}{\Lambda_1} \simeq \frac{2\pi}{L}\; F\left[(\beta - \beta_c)\; L^{1/\nu}\right]\,. \tag{26}$$

The best data collapse is obtained for the value (see Fig. 4):

$$\nu \simeq 1.1\,. \tag{27}$$

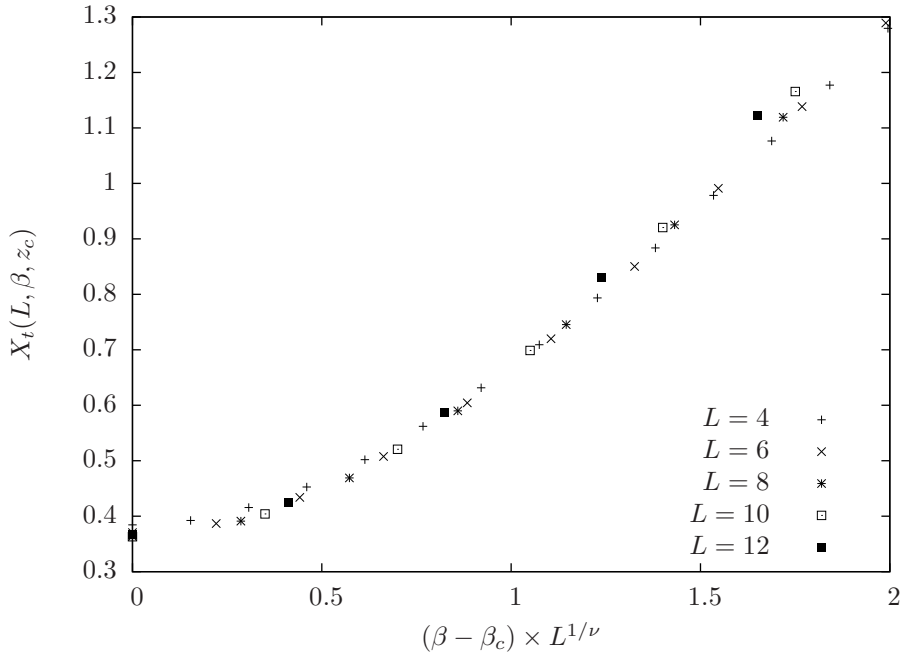

FIG. 4. Data collapse for the effective thermal exponent $X_t(L,\beta,z_c)$, under a perturbation of the parameter β. The value used for this plot is $1/\nu = 0.9$.

E. Relation to Hilbert-space truncation

We close this Section by comparing our approach to earlier studies[10,11] of the IQHE problem based on a different truncation procedure. Our method consists in writing the lattice path integral representation for the mean conductance using the supersymmetry trick, and then truncating the infinite sum over the paths, to keep only the self-avoiding paths. This gives us the well-defined loop model of Fig. 2, where we will tune slightly the Boltzmann weights to obtain an integrable point (see Section III).

In contrast, in[10,11], one starts from a two-dimensional single-particle Hamiltonian including Gaussian hopping coefficients, and computes its supersymmetric path integral. The resulting action is then interpreted as the action of a one-dimensional many-body supersymmetric Hamiltonian $H_{\rm MB}$, given in Eqs. (3–5) of[11]. This Hamiltonian is expressed in terms of the coefficients S^a of a superspin matrix. In this model, the Hilbert space for each site is infinite-dimensional (each site can be occupied by an arbitrary number of bosons). The idea is to truncate this Hilbert space down to dimension D, and follow the behaviour of the energy gap as D increases. The model is not critical for finite D, but it becomes critical in the limit $D\to\infty$.

Let us shown how to relate the terms of $H_{\rm MB}$ in the truncated space of dimension $D=5$, to the generators which encode the loop model of Fig. 2. We first get rid of the $(-1)^j$ factor in $H_{\rm MB}$[11]. This is done through the change

$$c_{\uparrow j}\to -c_{\uparrow j} \qquad \text{for } j\equiv 2 \mod 4 \quad \text{or} \quad j\equiv 3 \mod 4\,,$$

without affecting the (anti-)commutation relations for the b_j, c_j. We obtain the Hamiltonian:

$$H_{\rm MB}=\sum_{j=1}^{L}\left[\sum_{a=1}^{16} g_a S_j^a S_{j+1}^a+\eta(S_j^1+S_j^2+S_j^5+S_j^6)\right], \tag{28}$$

where the signs g_a are given by

$$g_a=\begin{cases}1 & \text{if } a=1,2,10,12,14,16\\ -1 & \text{if } a=3,\dots,9,11,13,15.\end{cases} \tag{29}$$

We decompose $H_{\rm MB}$ as a sum of generators

$$H_{\rm MB}=\sum_{j=1}^{L}\Big\{ -(\,{}^{\cup\!\cup})_j-(\,{}_{\cap\!\cap})_j+e_j+f_j+(1+\eta)\Big[(\rangle\quad)_j+(\quad\langle\!\langle)_j+2(\rangle\rangle\langle\!\langle)_j\Big]\Big\}, \tag{30}$$

where we have defined

$$\begin{aligned}
(\,{}^{\Cup}\,)_j &:= S^3_j S^3_{j+1} + S^7_j S^7_{j+1} + S^{15}_j S^{15}_{j+1} - S^{16}_j S^{16}_{j+1} \\
(\,{}_{\Cap}\,)_j &:= S^4_j S^4_{j+1} + S^8_j S^8_{j+1} + S^{13}_j S^{13}_{j+1} - S^{14}_j S^{14}_{j+1} \\
(\rangle\!\rangle\ \ )_j + (\rangle\!\rangle\,\langle\!\langle)_j &:= \tfrac{1}{2}\left(S^1_j + S^2_j + S^5_j + S^6_j\right) \\
(\ \ \langle\!\langle)_j + (\rangle\!\rangle\,\langle\!\langle)_j &:= \tfrac{1}{2}\left(S^1_{j+1} + S^2_{j+1} + S^5_{j+1} + S^6_{j+1}\right) \\
e_j &:= \left(S^1_j - \tfrac{1}{2}\right)\left(S^1_{j+1} - \tfrac{1}{2}\right) - \left(S^5_j + \tfrac{1}{2}\right)\left(S^5_{j+1} + \tfrac{1}{2}\right) + S^{10}_j S^{10}_{j+1} + S^{12}_j S^{12}_{j+1} \\
f_j &:= \left(S^2_j - \tfrac{1}{2}\right)\left(S^2_{j+1} - \tfrac{1}{2}\right) - \left(S^6_j + \tfrac{1}{2}\right)\left(S^6_{j+1} + \tfrac{1}{2}\right) - S^9_j S^9_{j+1} - S^{11}_j S^{11}_{j+1}\,.
\end{aligned} \tag{31}$$

In terms of the creation/annihilation operators, the above generators read:

$$\begin{aligned}
(\,{}^{\Cup}\,)_j &= (b^\dagger_{j\uparrow} b^\dagger_{j+1\uparrow} + c^\dagger_{j\uparrow} c^\dagger_{j+1\uparrow})(b^\dagger_{j\downarrow} b^\dagger_{j+1\downarrow} - c^\dagger_{j\downarrow} c^\dagger_{j+1\downarrow}) \\
(\,{}_{\Cap}\,)_j &= (b_{j\uparrow} b_{j+1\uparrow} + c_{j\uparrow} c_{j+1\uparrow})(b_{j\downarrow} b_{j+1\downarrow} - c_{j\downarrow} c_{j+1\downarrow}) \\
e_j &= (b^\dagger_{j\uparrow} b^\dagger_{j+1\uparrow} + c^\dagger_{j\uparrow} c^\dagger_{j+1\uparrow})(b_{j\uparrow} b_{j+1\uparrow} + c_{j\uparrow} c_{j+1\uparrow}) \\
f_j &= (b^\dagger_{j\downarrow} b^\dagger_{j+1\downarrow} - c^\dagger_{j\downarrow} c^\dagger_{j+1\downarrow})(b_{j\downarrow} b_{j+1\downarrow} - c_{j\downarrow} c_{j+1\downarrow}) \\
(\rangle\!\rangle\ \ )_j + (\rangle\!\rangle\,\langle\!\langle)_j &= \tfrac{1}{2}(b^\dagger_{j\uparrow} b_{j\uparrow} + c^\dagger_{j\uparrow} c_{j\uparrow} + b^\dagger_{j\downarrow} b_{j\downarrow} + c^\dagger_{j\downarrow} c_{j\downarrow}) \\
(\ \ \langle\!\langle)_j + (\rangle\!\rangle\,\langle\!\langle)_j &= \tfrac{1}{2}(b^\dagger_{j+1\uparrow} b_{j+1\uparrow} + c^\dagger_{j+1\uparrow} c_{j+1\uparrow} + b^\dagger_{j+1\downarrow} b_{j+1\downarrow} + c^\dagger_{j+1\downarrow} c_{j+1\downarrow})\,.
\end{aligned} \tag{32}$$

In the $D = 5$ truncated space, each site is either empty or occupied by two particles of opposite spins $(\uparrow, \downarrow)$. If each spin is interpreted as a loop color, the above generators (when restricted to the $D = 5$ space) obey a dilute two-color Temperley-Lieb algebra with loop weight $n = 0$. Hence, they represent the vertices u_1, u_2, w_1, x of the loop model defined in Section II C. In particular, the e_j and f_j form two decoupled Temperley-Lieb algebras.

Note that, in this context, the generator for the w_2 vertex, $E_j = e_j f_j$, cannot be realised by a linear combination of the $S^a_j S^a_{j+1}$, but it may be a linear combination of the $(S^a_j S^a_{j+1})^2$. So introducing E_j terms in the Hamiltonian leads to higher-order terms in $H_{\rm MB}$, and most probably it breaks the invariance with respect to the supersymmetric charges $Q_{1,2}$. However, we have shown that the supersymmetric model $H_{\rm MB}$, when restricted to the $D = 5$ space, corresponds to a particular manifold in the phase diagram of the two-color loop model.

III. CONSTRUCTION OF AN INTEGRABLE CRITICAL LOOP MODEL

In the preceding section, we truncated the the Chalker-Coddington network model to yield a two-color loop model that is simpler to analyze. To make further progress, we modify this model further. We augment it by allowing the "straight-line" vertices with weight v illustrated in Fig. 5. We also generalize it by allowing the weight per loop n to not only be zero, but to vary in the range $n \in [-2, 2]$. By utilizing the results of[28], we will show in this section that this modified model for all values of n in this range has an integrable line, and includes several critical points. The remainder of the paper will be devoted to the study of the critical behaviour.

When the straight-line vertices are allowed, the loop model can no longer be related directly to electron trajectories in a potential. In the original CC model, the 'checkerboard' structure of the lattice (or, equivalently, the alternation of arrows on the edges of $\mathcal{L}$) is essential to the interpretation of the paths as electron trajectories along the contour lines of the random potential. However, several arguments indicate that the truncated but unmodified loop model of Fig. 2 is in the same universality class as that of the modified model. In other words, one can obtain the unmodified model by perturbing the critical line with irrelevant operators.

One argument for the equivalence of the two stems from the relation of this two-color loop model to that studied in[20]. There the completely packed version was studied; in the notation used here this corresponds to setting the Boltzmann weights $t = u_1 = u_2 = v = 0$. It was shown that at least for weight per loop $n \geq \sqrt{2}$, the model has a critical point when x/w_2 is tuned appropriately. Moreover, at this critical point, numerical evidence strongly suggests that dilution (i.e. non-zero t, u_1 and u_2) is irrelevant. We will provide additional evidence by finding that for certain discrete values of $n \geq \sqrt{2}$, the critical point of the completely packed model and that of the modified model studied here are described by the same conformal field theory. Neither of these arguments applies when $n = 0$, but all the critical exponents we have computed $(X_t, X_{2,2}, \nu)$ for both the truncated CC model and the integrable model at $n = 0$ in regime 4 (see Table II) agree, up to our numerical precision. This strongly indicates that the integrable model at $n = 0$ in regime 4 is in the universality class of the truncated CC model.

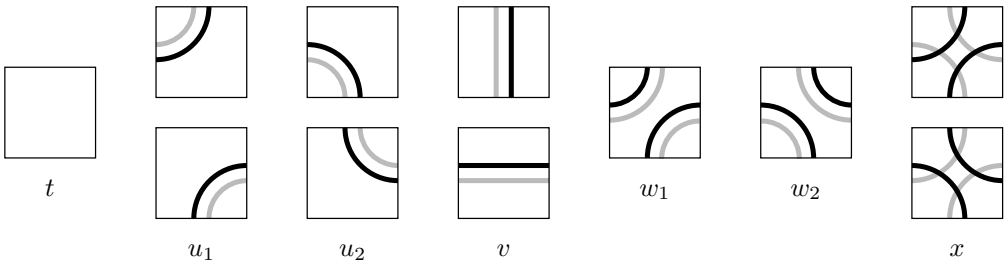

FIG. 5. Vertices of the augmented dilute two-color loop model.

In this section, we give the Boltzmann weights of the integrable critical line in the loop model of Fig. 5. These weights are expressed in terms of the generators of the dilute Birman-Wenzl-Murakami (dBWM) algebra, so that the solution of the Yang-Baxter equation found in[28] can be used. In Appendix A, we review the BWM algebra and its graphical presentation. The braid group can be represented in terms of the BWM generators, and can then be used to find invariants of knots and links generalizing the Jones polynomial[21].

An alternate way of obtaining the Boltzmann weights of the integrable critical line is to search for holomorphic observables on the lattice. These are operators whose expectation values satisfy the lattice analog of the Cauchy-Riemann equations. This method is described in Appendix B, and yields the same weights as those found in[28] using the dBWM algebra.

A. Critical completely packed loop models

We first review the critical completely packed loop model, arising for example in the Fortuin-Kasteleyn expansion of the Potts model[29]. Each vertex of this model has the two possible configurations displayed in Fig. 6. The partition

FIG. 6. Action of $\mathbf{1}$ (left) and e_j (right) on a pair of strands at positions j and $j+1$. The transfer matrix direction is upwards.

function is conveniently written in terms of the generators of the Temperley-Lieb (TL) algebra[30]. This algebra for a system of width L has L generators e_j acting at positions $j = 1, 2, \ldots, L$ as well as the identity $\mathbf{1}$, which obey the relations

$$e_j^2 = n\ e_j\,, \qquad e_j e_{j\pm1} e_j = e_j\,, \qquad e_i e_j = e_j e_i \quad \text{for } |i-j|>1. \tag{33}$$

The first of the relations encodes the fact that the weight for a closed loop is n, while the second encodes the fact that the weight does not depend on the length or the shape of the loop.

The Boltzmann weights of the integrable critical loop model are then

$$\check{R}_j(u) = \sin(2\theta - u)\,\mathbf{1} - \sin u\, e_j\,, \tag{34}$$

where $n = -2\cos 2\theta$ and $|n| \le 2$. The transfer matrix for an even number of sites L is then

$$T = \check{R}_1 \check{R}_3 \ldots \check{R}_{L-1} \check{R}_2 \check{R}_4 \ldots \check{R}_L\,. \tag{35}$$

It is straightforward to use the TL algebra to verify that these Boltzmann weights satisfy the Yang-Baxter equation

$$\check{R}_j(u)\check{R}_{j+1}(u+v)\check{R}_j(v) = \check{R}_{j+1}(v)\check{R}_j(u+v)\check{R}_{j+1}(u) \tag{36}$$

and the inversion relation

$$\check{R}_j(u)\check{R}_j(-u) = \sin(2\theta - u)\sin(2\theta + u)\ \mathbf{1}\,. \tag{37}$$

Braid group generators b_j and b_j^{-1} are found by taking $u \to \pm i\infty$:

$$\check{R}_j(i\infty) \propto b_j = e^{-i\theta}\,\mathbf{1} + e^{i\theta}\,e_j, \qquad \check{R}_j(-i\infty) \propto b_j^{-1} = e^{i\theta}\,\mathbf{1} + e^{-i\theta}\,e_j\ .$$

These satisfy the braid-group relations (A1) and (A2) as a consequence of the Yang-Baxter equation and the inversion relation respectively.

The critical completely packed loop model on the square lattice is in the same universality class as what is usually known as the O(n) model in its dense phase. Well-established results on the dense O(n) model[24] give the central charge of the CFT describing the scaling limit to be

$$c_{\mathrm{O}(n)} = 1 - \frac{3(\pi-2\theta)^2}{\pi\theta}\ . \tag{38}$$

The Boltzmann weights of the completely packed doubled loop model studied in[19,20] can be written in terms of the generators e_i and f_i of two independent TL algebras. This model is displayed in Fig. 5 with $t = u_1 = u_2 = v = 0$. In this picture, the e_j acts on black loops while the f_j act on grey loops, while the transfer matrix goes to the northeast. Thus the vertex with weight w_1 corresponds to the generator $\mathbf{1}$, the vertex with weight w_2 corresponds to e_jf_j, while those with weight x are e_j and f_j. Since the e_j's and the f_j's commute, we have immediately that the B_j, B_j^{-1} defined by

$$\begin{array}{rcl} B_j & := & \left(e^{-i\theta}\,\mathbf{1} + e^{i\theta}\,e_j\right)\left(e^{-i\theta}\,\mathbf{1} + e^{i\theta}\,f_j\right) \\ B_j^{-1} & := & \left(e^{i\theta}\,\mathbf{1} + e^{-i\theta}\,e_j\right)\left(e^{i\theta}\,\mathbf{1} + e^{-i\theta}\,f_j\right) \end{array} \tag{39}$$

also generate a braid group. Similarly, TL generators with loop weight $N = n^2$ may be constructed as

$$E_j := e_j\ f_j\,. \tag{40}$$

Using the relations (33) for the e_j's and f_j's, it is straightforward to show that the B_j, B_j^{-1}, E_j generate the BWM algebra described in Appendix A with parameters $N = n^2 = (-2\cos 2\theta)^2$, $\omega = e^{i6\theta}$ [20]. The doubled lines here correspond to the single lines displayed in Appendix A, as is apparent by comparing Figs. 5 and 14. Writing the Boltzmann weights in terms of this algebra is useful because solutions of the Yang-Baxter equation involving the BWM generators have long been known[31]. From this solution, a critical point for the coupled completely packed loop models for $n \geq \sqrt{2}$ was found[19,20]. With the parameterisation

$$n = 2\cos\frac{\pi}{r+2}\,,$$

in the isotropic case $w_1 = w_2$, the critical point is at $x/w_1 = \lambda_c$, where

$$\lambda_c = -\sqrt{2}\sin\left[\frac{\pi(r-2)}{4(r+2)}\right]\ . \tag{41}$$

At integer values $r = 2, 3, 4\ldots$, this critical point was identified with a particular conformal field theory, the WZW coset model $\mathrm{SU}(2)_r \times \mathrm{SU}(2)_r/\mathrm{SU}(2)_{2r}$. This conformal field theory has central charge

$$c_r = \frac{3r^2}{(r+1)(r+2)}\ . \tag{42}$$

For $1/\lambda_c < x/w_1 < \lambda_c$, the doubled loop model has a critical phase corresponding to two decoupled completely packed loop models. The central charge is thus twice (38).

B. The integrable critical line

We now can use the results of Grimm and Warnaar[28] to find an integrable model involving all the vertices in Fig. 5. We are interested mainly in the critical points, which can be written in terms of the dilute BWM algebra. The dilute BWM algebra extends the BWM algebra described in Appendix A to include edges of the lattice uncovered by strands. In the two-color loop model, these amount to allowing vertices to be empty of both colors. The dilute

generators act identically on the two colors, and so include the remaining vertices in Fig. 5. In an obvious notation, we then can write the $\check{R}$-matrix as

$$\begin{aligned}\check{R}_j(\varphi) = t(\varphi)(\ \ )_j + u_1(\varphi)\big[(\rangle\rangle\ \ )_j + (\ \ \langle\langle)_j\big] + u_2(\varphi)\big[(\cup\!\!\cup)_j + (\cap\!\!\cap)_j\big] \\ + v(\varphi)\big[(/\!\!/)_j + (\backslash\!\backslash)_j\big] + w_1(\varphi) I_j + w_2(\varphi) E_j + x(\varphi) X_j\,. \end{aligned} \tag{43}$$

In terms of the TL generators introduced in the previous section, $E_j = e_j f_j$ and $X_j \equiv e_j + f_j$, while I_j takes value 0 on the dilute configurations and 1 otherwise.

Since the non-dilute vertices satisfy the BWM algebra, it is simple to show that the operators

$$B_j, E_j, I_j, (\ \ )_j, (\rangle\rangle\ \ )_j, (\ \ \langle\langle)_j, (\cup\!\!\cup)_j, (\cap\!\!\cap)_j, (/\!\!/)_j, (\backslash\!\backslash)_j$$

constructed from the two-color loop model satisfy a dilute BWM algebra. Namely, with doubled lines here corresponding to single lines in Appendix A, and the B_j defined in (39), these operators generate the dilute BWM algebra with parameters $(N = (q+q^{-1})^2, \omega = q^3)$, where $q = e^{2i\theta}$.

In[28], an integrable model based on the dBWM algebra was derived. With $n = -2\cos 2\theta$ as before, its Boltzmann weights are given by

$$\begin{aligned} t(\varphi) &= -\cos(2\varphi - 3\theta) - \cos 5\theta + \cos 3\theta + \cos\theta \\ u_1(\varphi) &= -2\sin 2\theta \sin(\varphi - 3\theta) \\ u_2(\varphi) &= \ \ 2\sin 2\theta \sin\varphi \\ v(\varphi) &= -2\sin\varphi \sin(\varphi - 3\theta) \\ w_1(\varphi) &= \ \ 2\sin(\varphi - 2\theta)\sin(\varphi - 3\theta) \\ w_2(\varphi) &= \ \ 2\sin\varphi \sin(\varphi - \theta) \\ x(\varphi) &= \ \ 2\sin\varphi \sin(\varphi - 3\theta)\,. \end{aligned} \tag{44}$$

We denote by φ_0 the isotropic value which is closest to zero:

$$\varphi_0 = \begin{cases} \frac{3\theta}{2} & \text{if } 0 < \theta < \frac{\pi}{3} \\ \frac{3\theta}{2} - \pi & \text{if } \frac{\pi}{3} < \theta < \pi. \end{cases} \tag{45}$$

The universal properties are independent of the anisotropy parameter φ (as long as φ lies between 0 and φ_0), but depend very strongly on θ, as we shall see. At the isotropic point $\varphi = 3\theta/2$, the weights can be rescaled to

$$\begin{aligned} &t = 2\cos 3\theta + 2\cos 2\theta + 1 \\ &u_1 = u_2 = 4\cos\tfrac{\theta}{2}\cos\theta \\ &v = 2\cos\theta + 1 \\ &w_1 = w_2 = 1 \\ &x = -(2\cos\theta + 1)\,. \end{aligned} \tag{46}$$

The integrable model defined by (43)–(44) obeys the following properties:

- The isotropic weights are invariant under the transformations $\theta \to 2\pi + \theta$, and $\theta \to -\theta$, so the range of inequivalent couplings is $\theta \in [0, \pi]$. Each value of $n \in [-2, 2]$ appears twice in this interval.

- Since there are no loop ends, the number of loops mod 2 is the same as the number of x vertices mod 2. This allows us to change the sign of n by absorbing the sign in the weight x: $(n, x) \to (-n, -x)$. Thus there are four distinct critical points for each value of $n \in (0, 2)$, while there are two for $n = 0$ and $n = 2$.

- The weights satisfy the inversion relation

$$\check{R}(\varphi)\check{R}(-\varphi) = 4\sin(2\theta - \varphi)\sin(2\theta + \varphi)\sin(3\theta - \varphi)\sin(3\theta + \varphi)\ \mathbf{1}\,. \tag{47}$$

- Rotating by 90° is equivalent to sending $\varphi \to 3\theta - \varphi$.

- The weights are trivial when $u = 0$: $\check{R}(0) = 2\sin 2\theta \sin 3\theta\ \mathbf{1}$.

- The eigenvalues of the transfer matrix are preserved under $(u_1, u_2) \to (-u_1, -u_2)$ and $v \to -v$.

C. The quantum Hamiltonian

To gain intuition into this doubled loop model, it is useful to find the equivalent 1d quantum Hamiltonian by taking the very anisotropic limit $\varphi \to 0$. The Hamiltonian is found from the transfer matrix $T_L(\varphi)$ for L sites by

$$H := 2\sin 2\theta \sin 3\theta \left.\frac{\mathrm{d}\log T_L(\varphi)}{\mathrm{d}\varphi}\right|_{\varphi=0} + 2L\sin 5\theta \; \mathbf{1} \; ,$$

yielding

$$H = \sum_{j=1}^{L} \Big\{ 4\cos 4\theta \sin\theta \; (\quad)_j + 2\cos 2\theta \sin 3\theta \; [(\rangle\rangle \quad)_j + (\quad \langle\langle)_j] + 2\sin 2\theta \; [(\cup\!\!\cup)_j + (\cap\!\!\cap)_j]$$
$$+2\sin 3\theta \; [(/\!\!/)_j + (\backslash\!\backslash)_j] - 2\sin\theta \; E_j - 2\sin 3\theta \; X_j \Big\} . \tag{48}$$

To find the Fermi velocity v_f, we assume that in the scaling limit this Hamiltonian is that of a conformal field theory. In the next Section, we will present much evidence in support of this assumption. In a conformal field theory, the ground-state energy (the lowest eigenvalue of H) is[32]

$$E_L^0 \simeq L e_\infty - \frac{\pi c}{6L} \; v_f \, . \tag{49}$$

where c is the central charge. Let $\Lambda_L^0(\varphi)$ be the dominant eigenvalue of the transfer matrix. The analysis of Appendix B indicates that the free energy of the loop model on a rhombic lattice with angle α is given by $\left[-\log \Lambda_L^0(\varphi)\right]$, where $\alpha = \pi\varphi/(2\varphi_0)$ and φ_0 is the isotropic value, as defined in (45). In a conformal field theory, one expects[32]

$$-\log \Lambda_L^0(\varphi) \simeq L f_\infty(\alpha) - \frac{\pi c}{6L} \sin\alpha \, . \tag{50}$$

Differentiating (50) around $\varphi = 0$ and comparing with (49) yields

$$v_f = \left| \frac{2\pi \sin 2\theta \sin 3\theta}{2\varphi_0} \right| , \qquad \varphi_0 = \begin{cases} \frac{3\theta}{2} & \text{if } 0 < \theta < \frac{\pi}{3} \\ \frac{3\theta}{2} - \pi & \text{if } \frac{\pi}{3} < \theta < \pi. \end{cases} \tag{51}$$

IV. IDENTIFYING THE CRITICAL THEORIES

In this Section, we present what we believe is convincing evidence that the doubled loop model with Boltzmann weights (44) is critical. We find the presumably exact central charge of the conformal field theories describing the scaling limit, and also give some of the dimensions of fields. We do this by a combination of calculations exploiting the integrability, comparison to a similar integrable model, and exact diagonalization of the transfer matrix and the Hamiltonian for widths up to $L = 14$ sites.

A. The four regimes

This critical line is parametrized by the value of $\theta \in [0, \pi]$, related the weight per loop by $n = -2\cos 2\theta$. Since the Fermi velocity vanishes at $\theta = \frac{\pi}{3}, \frac{\pi}{2}$, and has a discontinuity at $\theta = \frac{2\pi}{3}$, it is natural to expect that the physics is discontinuous if θ is varied across these values. We thus divide the critical line into four regimes, as described in Table II.

All known integrable models with Boltzmann weights parameterized by trigonometric functions of the anisotropy parameter φ are critical, and this is no exception. One argument for this is the existence of the lattice holomorphic operator described in Appendix B. Another is the inversion-relation calculation done below, which shows that with standard assumptions about holomorphicity in φ, the free energy is singular as this critical point. A numerical check is to use exact diagonalization to find the largest eigenvalue of T and/or the ground-state energy of H, and then fit the results to (49) or (50). To extract the central charge c, we use two different-length systems to get rid of the extensive piece Le_∞. Doing this, we find the results given in Fig. 7. We see a very nice convergence to the critical behavior as expected.

regime	θ-range	parameterisation	central charge
1	$0 < \theta < \frac{\pi}{3}$	$n = -2\cos\frac{\pi}{r+2}$	$c = 2\left[1 - \frac{6}{(r+1)(r+2)}\right] + \frac{1}{2}$
2	$\frac{\pi}{3} < \theta < \frac{\pi}{2}$	$n = \quad 2\cos\frac{\pi}{r+2}$	$c = 2\left[1 - \frac{6}{(r+1)(r+2)}\right]$
3	$\frac{\pi}{2} < \theta < \frac{2\pi}{3}$	$n = \quad 2\cos\frac{\pi}{r+2}$	$c = \frac{3r^2}{(r+1)(r+2)} + \frac{1}{2}$
4	$\frac{2\pi}{3} < \theta < \pi$	$n = -2\cos\frac{\pi}{r+2}$	$c = \frac{3r^2}{(r+1)(r+2)}$

TABLE II. The four regimes of the integrable loop model.

We combine these results with other arguments to conjecture exact formulae for the central charge for all θ. We can also identify precisely which conformal field theories describe some critical lines. There are two types of conformal field theories known to describe doubled loop models, and both occur along this critical line. Unfortunately, the value of $n = 0$ at $\theta = \frac{3\pi}{4}$ of interest for the truncated CC model lies in one of the regions where we do not understand the conformal field theory. As is apparent from Fig. 7, we do know that $c = 0$ as required there.

At several special values of θ, the model simplifies. Namely, when $n = \pm 1$, all loop configurations receive the same weight (if $n = -1$, we transform $(n, x) \to (-n, -x)$ as explained in Sec. III B). Thus when computing the partition function, we can sum up the four completely packed vertices to give a single one with weight $w_1 + w_2 + 2nx$.

For $\theta = \frac{2\pi}{3}$ at the isotropic point, $x = v = 0$, so this reduces to a six-vertex model with no staggering. Here the usual parameter[33] has value

$$\Delta = \frac{a^2 + b^2 - c^2}{2ab} = -1\,,$$

so this is in the same universality class as the antiferromagnetic Heisenberg model. Thus the central charge is $c = 1$ and the first thermal exponent is $X_t = \frac{1}{2}$, in agreement with the numerical results in Figs. 7–8.

At $\theta = \frac{\pi}{6}$ and $\theta = \frac{5\pi}{6}$, we obtain a staggered version of the eight-vertex model. Ordinarily the staggered eight-vertex model is not solvable, but as we detail in Appendix C, this one is not only solvable, but can be mapped onto a free-fermion theory. There we show that there are two Majorana fermions present, but only one of the two is critical. Thus the central charge is $c = \frac{1}{2}$ here, again consistent with the numerics.

B. Computation of an exact scaling dimension

Since the model is integrable, it is possible to derive some quantities exactly. Here we extract the dimension of an operator in the critical theory as a function of θ. This is possible because at certain discrete values of θ, there exists a deformation away from the critical point preserving the integrability[28]. The inversion-relation method[33] yields the free energy along this deformation, and by analyzing its expansion around the critical point, we extract the value of the exponent $\nu_{\rm int}$. This then yields the dimension of the operator which when added to the action causes the deformation.

It is convenient to parameterize the loop weight n within each of the four regimes by a parameter r,

$$n = 2\epsilon\cos\frac{\pi}{r+2}\,, \tag{52}$$

where $\epsilon = -1$ in regimes 1 and 4, and $\epsilon = 1$ in regimes 2 and 3 (see Table II).

The integrable deformations resulting in unitary field theories occur at integer values of r in all four regimes. Here the dilute BWM algebra admits a "height" or "Restricted Solid-On-Solid" (RSOS) realization[28]. Instead of treating the loops as the degrees of freedom, on the dual lattice one places height variables, which are integers restricted to a certain interval. The loops then play the role of domain walls separating regions of different heights.

The inversion-relation method is a way of computing the free energy exactly after making assumptions about its holomorphicity properties as a function of φ. The free energy satisfies constraints following from the inversion relation

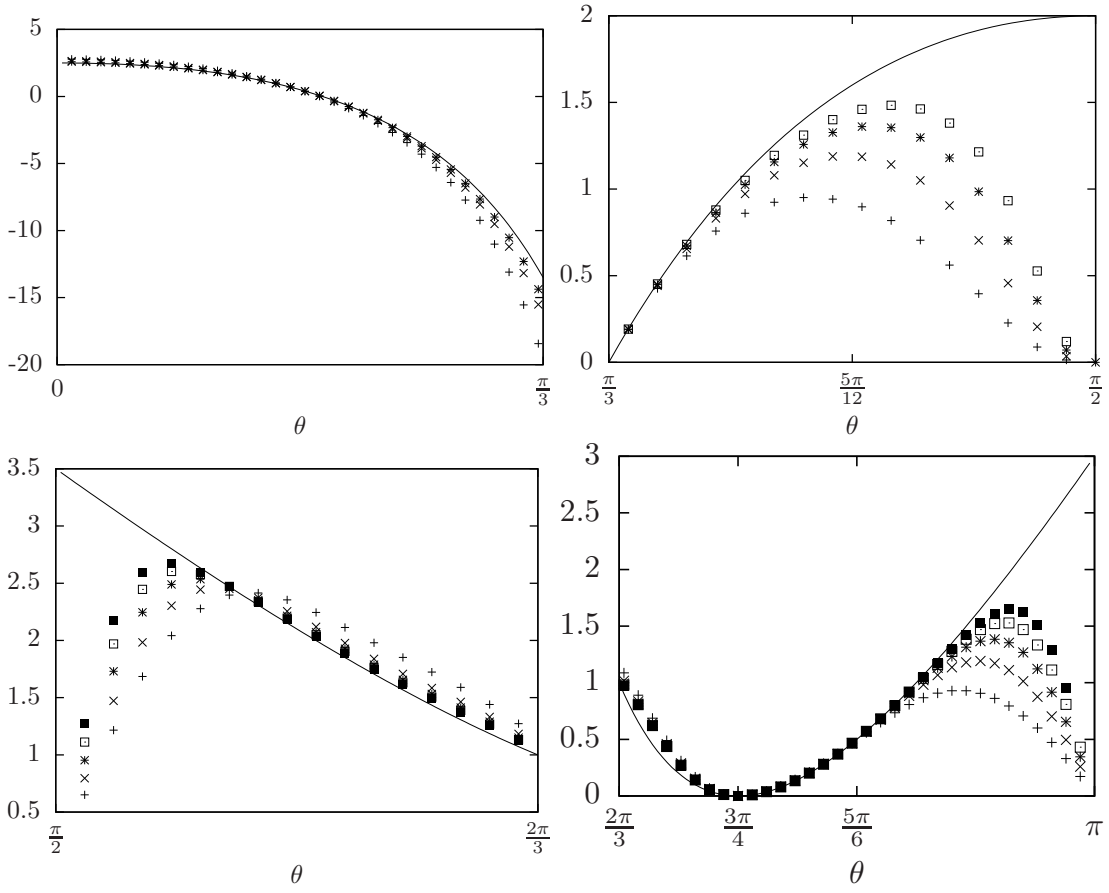

FIG. 7. Numerical estimates for the central charge in the four critical regimes. Different symbols represent data points for consecutive system sizes: $L = 4, 6$ $(+), L = 6, 8$ $(\times), L = 8, 10$ $(*), L = 10, 12$ $(\square), L = 12, 14$ $(\blacksquare)$. Full lines represent the predicted exact values from Table II.

(53) below, and the fact that sending $\varphi \to 3\theta - \varphi$ rotates the lattice by 90°. The holomorphicity assumptions then give a unique solution to these constraints. Parameterizing the deformation in our case by p, the inversion relation becomes[28]

$$\check{R}(\varphi, p)\check{R}(-\varphi, p) = (4p)^{-1}\,\theta_1(2\theta - \varphi, p)\,\theta_1(2\theta + \varphi, p)\,\theta_1(3\theta - \varphi, p)\,\theta_1(3\theta + \varphi, p)\;\mathbf{1}\,, \tag{53}$$

where $\theta_1(u, p)$ is the standard elliptic theta function. This indeed reduces to (47) in the critical limit $p \to 0$. From this, it is simple to show that the inverse of the transfer matrix in the diagonal direction is given by forming a transfer matrix out of products of $\check{R}_j(-\varphi, p)$.

Conveniently, both (53) and the behavior under rotational symmetry are identical to that of the model studied in[34], so we utilize these results. The singular part of the free energy approaching the critical point depends on p as $f_{\rm sing} \sim p^{2-\nu_{\rm int}}$, so the operator perturbing the critical theory in the integrable direction has scaling dimension $X_{\rm int} = 2 - 2/\nu_{\rm int}$. Then we find

$$X_{\rm int} = \begin{cases} \frac{r-1}{r+2} + 1 & \text{in regime 1,} \\ \frac{r-1}{r+2} & \text{in regime 2,} \\ \frac{3}{r+2} + 1 & \text{in regime 3,} \\ \frac{3}{r+2} & \text{in regime 4.} \end{cases} \tag{54}$$

We have written these results in terms of r instead of θ to emphasize that the derivation only applies to r integer, since this is where (53) can be derived. However, we expect that the results can be continued to all r within a given regime, since the equations themselves depend on r as a continuous parameter.

A good check of the validity of (54) for generic θ is that it corresponds exactly to $X_{\rm int} = 2s$, where s is the spin of the discretely holomorphic parafermion $\psi_s(z)$ described in Appendix B: see (B6).

C. Description by conformal field theory

Here we give formulae for the central charges in all four regimes that are presumably exact. All are related to those occurring in completely packed models. However, the doubled loop models are not identical to completely packed models: we have checked that the doubled loops have non-trivial fractal dimension in regime 4 (see Section V C).

One type of critical behavior possible for a doubled loop model is simply to have the two colors decouple in the scaling limit. This occurs in the isotropic completely packed version when $x = -w_1 = -w_2$, and is argued to persist in a region around this point[20]. The central charge is simply twice $c_{O(n)}$ given in (38). Examining our numerical results for c, we see that in regime 2, the central charge indeed is converging nicely to $2c_{O(n)}$ with the appropriate dependence on n. When r is an integer, this is twice the central charge of the conformal minimal models, and so the corresponding height model should scale to two decoupled minimal models. An additional check on this comes from the fact that the dimension of the integrable perturbing operator in (54) is twice that of an operator in a minimal model. Namely, we have $X_{\rm int} = 2X_{1,2}$, where $X_{1,2} = \frac{r-1}{2(r+2)}$ is the scaling dimension of the $\Phi_{1,2}$ operator in the minimal model with central charge $c = 1 - \frac{6}{(r+1)(r+2)}$. It is thus natural to conjecture that in regime 2, the scaling limit of our integrable loop model is indeed that of two decoupled completely packed loop models. These conformal field theories have been extensively studied[35].

In regime 1, the numerics for the central charge are apparently converging to $2c_{O(n)} + \frac{1}{2}$. Thus here the loops apparently decouple as well, but additional critical Ising degrees of freedom appear. This is consistent with the mapping to the Ising model at $\theta = \frac{\pi}{6}$ described in Appendix C. The scaling dimension $X_{\rm int}$ here is $2X_{1,2} + 1$, leading to the natural interpretation that the operator is a product of the $\Phi_{1,2}$ operators in the two minimal models with the energy operator in the Ising model, the latter having dimension 1. These extra Ising degrees of freedom, which also occur in a certain regime of the square-lattice O(n) model[36], appear through the following mechanism. The vertices of the loop model obey a $\mathbb{Z}_2$ symmetry, in the sense that any vertex is surrounded by an even number of empty edges. Thus empty edges form polygons where each node has even degree, and so they respect the geometry of Ising domain walls for Ising variables σ lying on the dual lattice. Depending on the values of the Boltzmann weights, these Ising variables may become critical in the continuum limit. This is evidently what happens in regime 1.

The critical behavior in regimes 3 and 4 is not that of two decoupled models. As mentioned above in Sec. III A, in the completely packed version of the doubled loop model, there occurs a coupled critical point corresponding to the $\mathrm{SU}_r(2) \times \mathrm{SU}_r(2)/\mathrm{SU}_{2r}(2)$ WZW coset model, with central charge c_r (42). The numerical analysis in Fig. 7 nicely fits to c_r in regime 4, and agrees with the Ising value $c = \frac{1}{2}$ at $\theta = \frac{5\pi}{6}$, derived in Appendix C. Moreover, when r is an integer, the exponent $X_{\rm int}$ in (54) belongs to the above coset theory. Thus it is natural to conjecture that the central charge throughout regime 4 is c_r. As we see from our numerics at $n = 0$ (see Sec. V C), the fractal dimension of a single loop is $d_f < 2$, so regime 4 represents a "dilute branch" of the coset theory.

Likewise, in regime 3 the data seem to be converging to $c_r + \frac{1}{2}$, agreeing with the six-vertex value $c = 1$ at $\theta = \frac{2\pi}{3}$. The exponent $X_{\rm int}$ is 1 greater than the value in regime 4, so it is natural to interpret that the operator is multiplied by the Ising energy operator of dimension of 1. Thus like in regime 1, the critical theory presumably includes an extra Ising piece.

Outside r integer, the conformal field theory in regimes 3 and 4 is not understood. Moreover, we will see in the subsequent section that even though the formula for the central charge is applicable for all r, it is not even clear whether dimensions of exponents can be continued to values of $|n| < 1$.

V. CRITICAL BEHAVIOUR IN REGIME 4

The main motivation of this paper is to explore a doubled loop model arising in the truncation of the Chalker-Coddington network model. For a connection to disordered systems, the weight per loop n and the central charge c must be zero. We have two $n = 0$ points, but for $\theta = \frac{\pi}{4}$ inside regime 1, the corresponding critical field theory seems to have nothing to do with the CC model. Not only do the different colors of loop decouple, but the extra Ising degree of freedom makes $c \neq 0$. We thus in this section focus on the behavior in regime 4, which contains the other $n = 0$ point at $\theta = \frac{3\pi}{4}$.

As noted above, we do not have a conformal field theory description valid in regime 4 outside of integer r. It therefore seems a good idea to exploit the fact that the associated height description at these points is described by the coset conformal field theory $\mathrm{SU}(2)_r \times \mathrm{SU}(2)_r/\mathrm{SU}(2)_{2r}$.

A. Integrable perturbations

This coset theory is known to have two integrable perturbations. One of them, found by using level-rank duality on the results of[37], is by the operator with dimension $X_{\rm int} = \frac{3}{r+2}$ discussed above. This perturbation describes the scaling limit of the height model with elliptic Boltzmann weights[28]. In terms of the loop model, we have found that the discrete parafermion $\psi_s(z)$ of Appendix B is the chiral part of the corresponding operator. This parafermion consists of the insertion of a one-leg defect for each loop flavour.

The other integrable perturbation also has a very natural meaning in terms of loops. This perturbing operator corresponds to the (1,1;adjoint) operator of dimension $X_{(1,1;\rm adj)} = \frac{2r}{r+1}$. Several arguments imply that this perturbation corresponds to changing the weight per unit length of the loops[38]. This integrable field theory describes the scaling limit of an integrable height model[39], and using the BWM algebra, it is described in[38] how to relate this height model to a dilute doubled loop model very similar to the one we study here. Moving away from the critical point in this similar model turns out to be effectively changing the weight per unit length. The second argument implying this result involves the S matrices for this integrable field theory, which decompose into the tensor product of S matrices of two minimal models $\mathcal{S}_r \times \mathcal{S}_r$[40]. It is natural to interpret the worldlines of a particle in a single minimal model as a loop in the O(n) model[41]. Thus when the S matrix is given by this tensor product, it is natural to interpret the worldlines of such particles as doubled loops; when two particles scatter they obey one of the four processes in the vertices w_1, w_2 and x pictured in Fig. 5. In such an interpretation, the weight per unit length of the loop is related to the mass of the particle. In the field theory, moving along this integrable line corresponds precisely to varying the mass of the particle.

We denote X_t the thermal exponent, defined as the conformal dimension for the first excited state in the zero-leg sector. The numerical calculation of X_t (see Fig. 8) brings two observations. In the region $\frac{5\pi}{6} \lesssim \theta < \pi$, the thermal exponent X_t converges to $X_{(1,1;\rm adj)} = \frac{2r}{r+1}$ even for generic values of θ, whereas $X_{(1,1;\rm adj)}$ was derived only for integer values of r. This indicates that the results from the $\mathrm{SU}(2)_r \times \mathrm{SU}(2)_r/\mathrm{SU}(2)_{2r}$ coset WZW model may be continued to arbitrary $\frac{5\pi}{6} \lesssim \theta < \pi$. However, in the region $\frac{2\pi}{3} < \theta \lesssim \frac{5\pi}{6}$, X_t clearly deviates from the continued value $\frac{2r}{r+1}$: this shows that not all exponents of the loop model are given by analytic continuation of the WZW coset model in this region, including our point of interest $\theta = \frac{3\pi}{4}$.

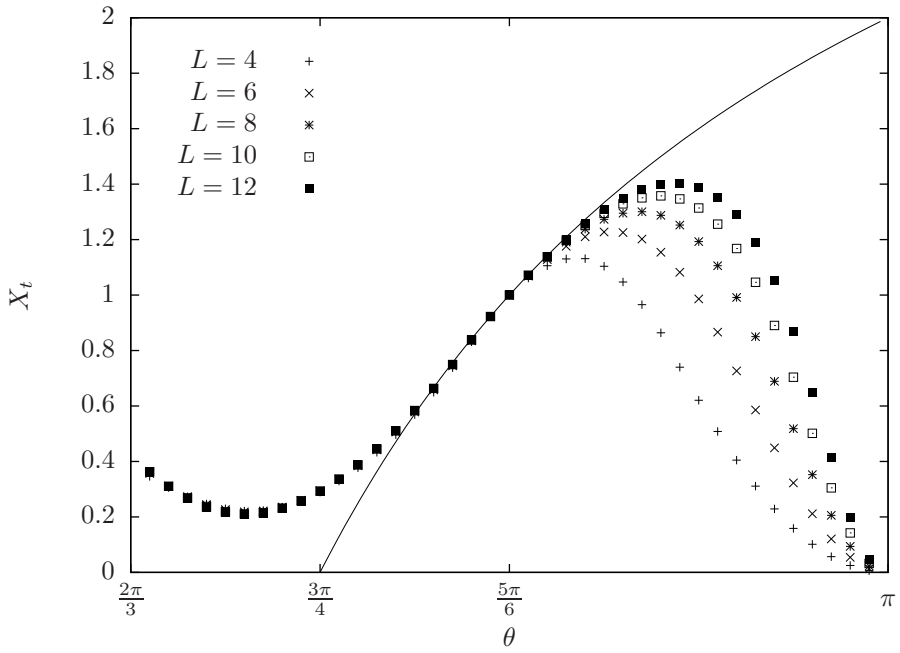

FIG. 8. Thermal exponent X_t in regime 4. Data points were obtained by transfer-matrix diagonalisation, and the solid line represents the exact result for the integrable perturbation dimension $X_{(1,1;\rm adj)} = \frac{2r}{r+1}$.

B. Correlation length exponent ν

The correlation length exponent ν is defined as the analog for the loop model of $\nu_{\rm CC}$ (4). In the CC model, the effect of perturbing the energy level E away from the transition value E_c amounts to taking β, β' out of the critical line (17). The analog of this perturbation in the integrable loop model is to introduce a staggering of the spectral parameter between the even and odd sublattices, with symmetric values around the isotropic spectral parameter φ_0 (51): $\varphi = (1 \pm \lambda)\varphi_0$, in the range $-1 \leq \lambda \leq 1$.

The parameter λ acts in a similar way to $(\beta - \beta_c)$ in the original CC model. At $\lambda = -1$, the only allowed loops are those with minimal length, winding around the vertices of one sublattice (say, the even one). At $\lambda = 1$ loops also have minimal length, but wind around the odd sublattice. The critical transition takes place at $\lambda = 0$, where the two sublattices become equivalent, and loops may be very long. In the limit $\lambda \to 0$, we expect this perturbation to develop a correlation length, scaling as

$$\xi \sim |\lambda|^{-\nu} \,. \tag{55}$$

Since this staggering does not respect the rapidity lines of the square lattice, it breaks integrability.

Let us first discuss the point $\theta = \frac{5\pi}{6}$, where the model maps to free fermions and remains solvable when the λ perturbation is included (see Appendix C). At this point, we get the analytical result $\nu = 2$, whereas the energy operator of the free-fermion theory is $X_t = 1$. In Appendix C, we show that the effective theory is a massive Majorana fermion with mass proportional to λ^2 and not λ. Thus, at $\theta = \frac{5\pi}{6}$, we have the relation between ν and the dimension of the perturbing operator:

$$X_t = 2 - \frac{2}{\nu} \,. \tag{56}$$

It is natural to assume that both ν and X_t are continuous in θ, so the effective mass term should still be proportional to λ^2 outside $\theta = \frac{5\pi}{6}$, and the relation (56) holds all along regime 4.

For $\theta \neq \frac{5\pi}{6}$, exponent ν is only accessible numerically, through finite-size scaling. The correlation-length exponent ν is obtained by assuming a one-parameter scaling law for the energy gap in the presence of the staggered perturbation λ. For $\lambda \simeq 0$, we expect the behaviour:

$$\log \frac{\Lambda_0(\lambda)}{\Lambda_1(\lambda)} \simeq \frac{2\pi}{L} F\left(\lambda \, L^{1/\nu}\right) \,, \tag{57}$$

where F is a scaling function. Since eigenvalues are unchanged under $\lambda \to -\lambda$, F must be an even function. In particular, at $\theta = \frac{3\pi}{4}$, like for the truncated CC model (see Sec. II D), we get the best data collapse (see Fig. 9) for the value

$$\nu \simeq 1.1 \,. \tag{58}$$

To our numerical precision, this value is close to what one would get from (56) with $X_t \simeq 0.3$. This is an indication that the relation (56) should hold throughout regime 4.

C. Other exponents

A finite-size scaling plot of the gap corresponding to $\ell_1 = \ell_2 = 1$ is shown in Fig. 10. The fact that it scales to zero faster than $1/L$ indicates that $X_{1,1}$, and hence $X_{|G|^2}$, are consistent with zero. In the untruncated CC model, the vanishing of the analogous exponent $X^{\rm CC}_{|G|^2}$ is due to probability conservation (see Sec. II D), but as far as we know there is no fundamental reason for this property to hold also in the truncated model, and it would be interesting to investigate this further. The observed slope in Fig. 10 suggests existence of an irrelevant operator with scaling dimension ≈ 3.2.

Moreover, we observe numerically that $X_t = X_{2,2}$. Hence, like for usual dilute polymers, this means that X_t is associated to a perturbation of the monomer fugacity (but different from the coset-model continuation to $r = 0$, which would yield $X_{(1,1;\mathrm{adj})} = 0$), and the fractal dimension of a path is

$$d_f = 2 - X_{2,2} \simeq 1.71 \,. \tag{59}$$

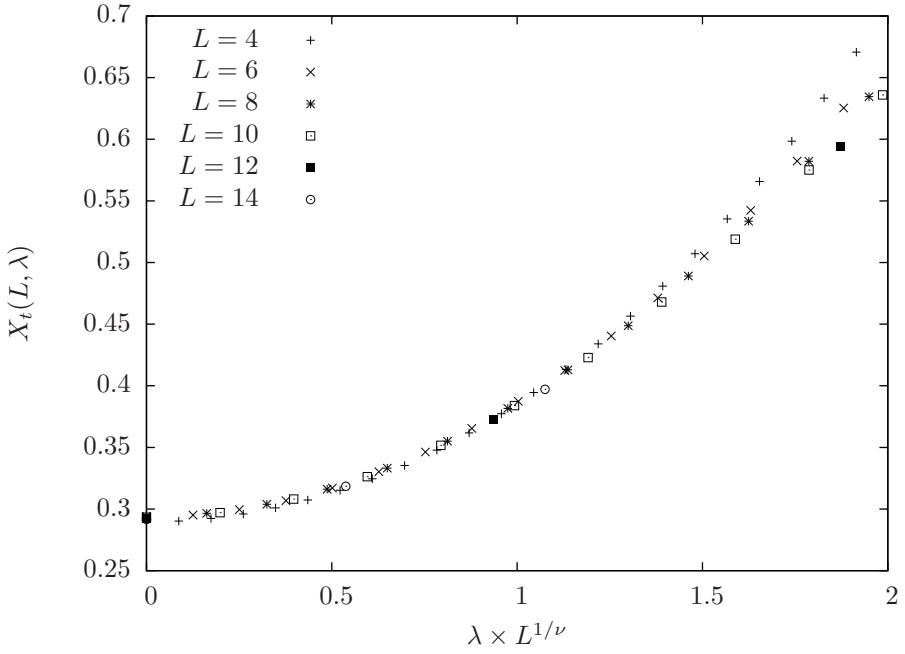

FIG. 9. Data collapse for the effective thermal exponent $X_t(L, \lambda)$ in the presence of a λ perturbation. The value used for this plot is $1/\nu = 0.9$.

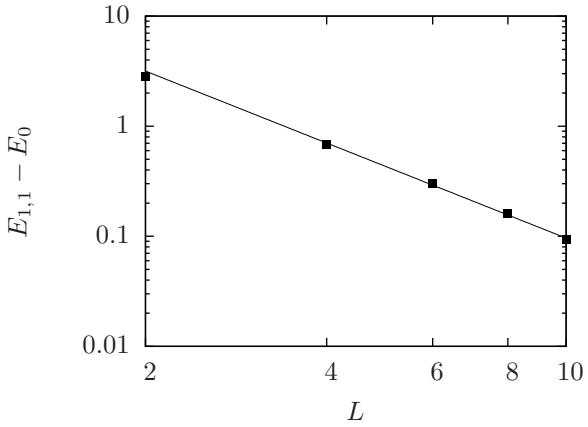

FIG. 10. Log-log plot of the energy gap for the watermelon $(1, 1)$ sector. Data points are fitted by a line of slope $\simeq -2.2$, and hence the conformal dimension is $X_{1,1} = 0$.

VI. DISCUSSION

Regimes 3 and 4 of the integrable model are particularly interesting, as the two loop colours remain coupled in the continuum limit. They are described by the "dilute branch" of the $\mathrm{SU}(2)_r \times \mathrm{SU}(2)_r/\mathrm{SU}(2)_{2r}$ WZW coset CFT (the same CFT as for the completely packed case[20]), with an additional Ising degree of freedom in regime 3. Strictly speaking, this theory is only valid at the RSOS points, but some critical properties (including the central charge) extend to the loop model for generic fugacity n. However, differences between the loop and RSOS spectra exist, as shown by our results on the thermal exponent X_t. An analytic study of the loop model through the Bethe Ansatz Equations is considered for future work. One also needs to understand if a Coulomb-Gas construction (most probably with a three-dimensional target space) could reproduce the coset results for generic n.

The original motivation for the present work was to propose an exactly solvable approximation to the IQHE transition. Unfortunately, our results for the correlation-length exponent ν clearly indicate that the point $n = 0$ of the integrable model is not in the universality class of IQHE. However, this model is a critical, integrable point in the

phase diagram of our modified CC model. It should really be considered as the first order in a hierarchy of truncated models, converging to the IQHE universality class. Higher-order truncated models should also contain integrable points, which may be built by "fusing" the edges of the first-order model, following[39] or a more recent approach based on additional $\mathbb{Z}_N$ symmetry[42].

From the numerical point of view, we used the only known efficient method to study a generic loop model: transfer-matrix diagonalisation. However, the inherent limitations on the system size prevent us from obtaining sharp estimates for the exponents, especially for ν. Recently, new Monte-Carlo algorithms have been proposed to simulate 2d loop models[43]. We hope to adapt this new approach to two-colour models, and get more precise estimates for the exponents of our truncated CC model.

ACKNOWLEDGMENTS

The work of P.F. was supported in part by NSF grants DMR/MPS 1006549 and 0704666. The work of Y.I. is supported by the European Research Council (grant CONFRA 228046).

Appendix A: The BWM algebra

In this Appendix, we recall the motivation and definition of the BWM algebra in a graphical language.

The BWM algebra[21] is a braid-monoid algebra, an object relevant to knot theory. It was originally designed to compute a certain *link invariant*, and later it was realised that it could be represented by RSOS models related to affine Lie algebras[31]. In[28], a dilute version of the BWM algebra was constructed, together with the corresponding R-matrix.

In the context of knot theory, the basic objects under consideration are *braids*. Let $(p_1, \ldots, p_L)$ be L distinct points in the complex plane, and define two copies of each point in three-dimensional space, $p'_j = p_j \times \{0\}, p''_j = p_j \times \{1\}$, so that the points $\{p'_j\}$ and $\{p''_j\}$ lie in two parallel planes. For all $j = 1, \ldots, L$, take a curve Γ_j enclosed between the two planes, and connecting p'_j to p''_j. Furthermore, impose that the Γ_j's do not intersect each other. Denote the multiplet $\Gamma = (\Gamma_1, \ldots, \Gamma_L)$: a braid β is then an equivalence class of Γ's, *modulo* continuous deformations of the curves. A typical braid is depicted in Fig. 11.

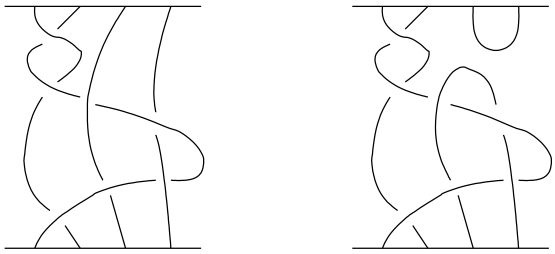

FIG. 11. An element of the braid group (left) and a word of the braid-monoid algebra (right) for $L = 4$.

Multiplication of two braids β, β' is defined by the concatenation of the two corresponding diagrams, with the convention that diagrams act from bottom to top: the product $\beta\beta'$ corresponds to β above β'. The β's form the braid group, generated by the elementary braids B_j, B_j^{-1}, which satisfy the relations:

$$B_j B_j^{-1} = B_j^{-1} B_j = \mathbf{1} \tag{A1}$$

$$B_j B_{j+1} B_j = B_{j+1} B_j B_{j+1} \tag{A2}$$

$$B_j B_\ell = B_\ell B_j \qquad \text{if } |j - \ell| \geq 2. \tag{A3}$$

Consider now multiplets $\Gamma = (\Gamma_1, \ldots, \Gamma_L)$ of non-intersecting curves connecting all the elements of $\{p'_j\} \cup \{p''_j\}$, without the restriction that a curve should go from a p'_j to a p''_k. The corresponding diagrams are then words on the alphabet $\{B_j, B_j^{-1}, E_j,\ j = 1, \ldots, (L-1)\}$, where the meaning of the letters B_j, B_j^{-1}, E_j is given in Fig. 12. The algebra on these words is called a braid-monoid algebra. It has two parameters (N, ω), and is defined by the

braid-group relations (A1)–(A2), together with the additional relations (see Fig. 13):

$$E_j^2 = N\ E_j \tag{A4}$$
$$E_j E_{j\pm1} E_j = E_j \tag{A5}$$
$$B_j E_j = E_j B_j = \omega\ E_j \tag{A6}$$
$$B_j B_{j\pm1} E_j = E_{j\pm1} B_j B_{j\pm1} = E_{j\pm1} E_j\ . \tag{A7}$$

Equations (A4)–(A5) mean that the E_j form a Temperley-Lieb algebra with loop weight N.

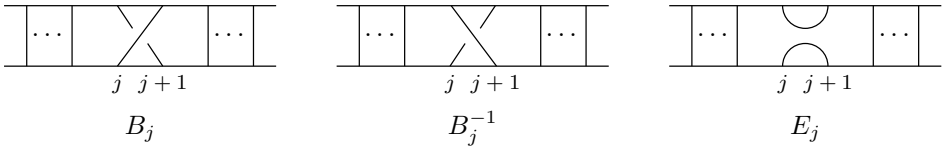

B_j B_j^{-1} E_j

FIG. 12. Generators of a braid-monoid algebra.

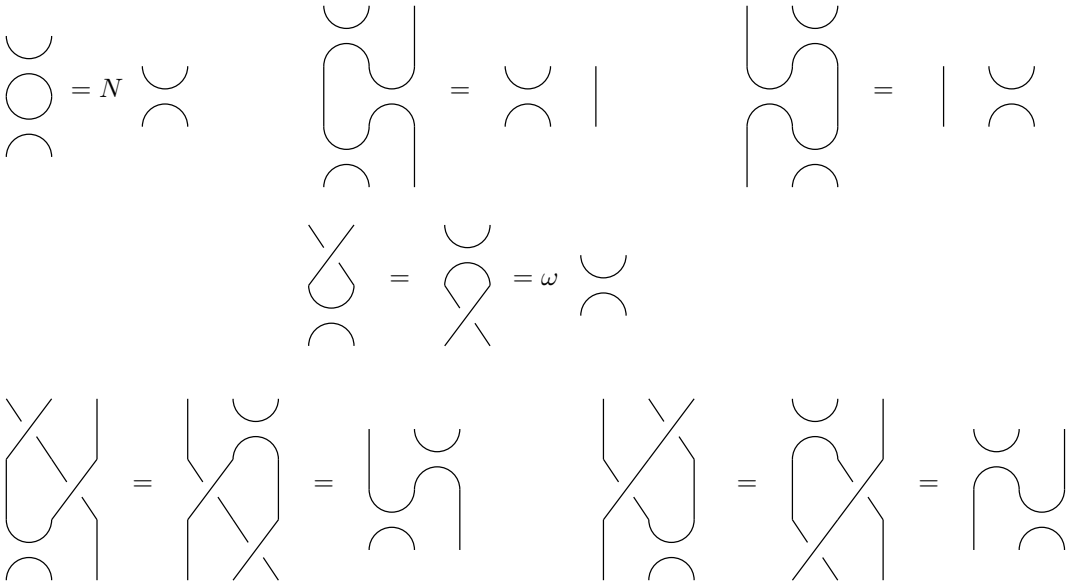

FIG. 13. Algebraic rules in the braid-monoid algebra with parameters (N, ω).

The BWM algebra is a braid-monoid algebra (A1)–(A7) where one imposes a linear relation between B_j, B_j^{-1} and E_j:

$$E_j = \mathbf{1} + \frac{B_j - B_j^{-1}}{q - q^{-1}}\,, \qquad \text{where} \quad N = 1 + \frac{\omega - \omega^{-1}}{q - q^{-1}}\,. \tag{A8}$$

The reason for introducing such a constraint is that the resulting algebra supports a linear form (the Markov trace) which is identical to a geometric invariant of the diagrams Γ (the Kauffman polynomial)[21].

The dBWM algebra[28] is obtained by allowing vacancies, or equivalently by taking multiplets of curves $\Gamma = (\Gamma_1, \ldots, \Gamma_\ell)$ with $0 \le \ell \le L$. This amounts to adding the generators

$$I_j, (\ \ )_j, (\rangle\ )_j, (\ \langle)_j, (^{\cup})_j, (_{\cap})_j, (/)_j, (\backslash)_j,$$

whose action is depicted in Fig. 14. In equations (A1) and (A8), $\mathbf{1}$ is replaced by I_j, so that the B_j, B_j^{-1}, E_j still form a BWM algebra on the set of occupied sites. Additional relations for the dilute generators should be included, to implement invariance under continuous deformation of the curves in the presence of vacancies. The full set of dBWM relations is given in[28].

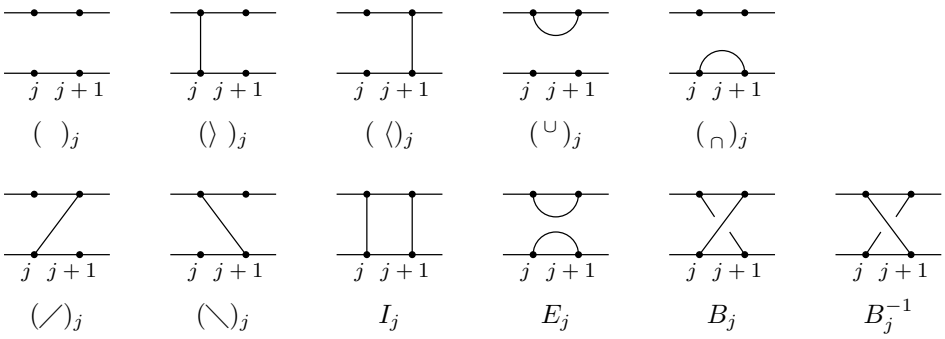

FIG. 14. The generators of the dilute BWM algebra.

Appendix B: Discretely holomorphic parafermion in the loop model

In this Appendix, we show that the two-colour loop model admits a discretely holomorphic parafermion $\psi_s(z)$[44–46] exactly on the integrable manifold (44). The parafermion $\psi_s(z)$ is defined on the midpoints of the dual lattice $\mathcal{L}^*$, and inserts a one-leg defect for each color at point z. In the two-point function $\langle\psi_s(0)\psi_s(z)\rangle$, there is a black (resp. grey) path γ_1 (resp. γ_2) connecting 0 and z, and one includes a phase factor involving the winding angles W of the paths γ_1, γ_2:

$$\langle\psi_s(0)\psi_s(z)\rangle = \frac{1}{Z}\sum_{(\gamma_1,\gamma_2)_{0\to z}}\ \sum_{C|(\gamma_1,\gamma_2)} \Pi(C)\ e^{\frac{is}{2}[W(\gamma_1)+W(\gamma_2)]}\,, \tag{B1}$$

where the first sum is over all possible pairs of paths from 0 to z, the second sum is over the loop configurations C compatible with γ_1 and γ_2, and $\Pi(C)$ is the Boltzmann weight for a loop configuration C.

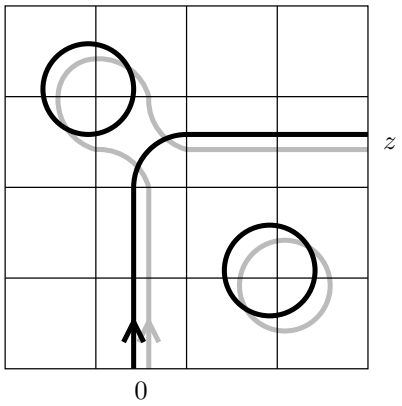

FIG. 15. A loop configuration contributing to $\langle\psi_s(0)\psi_s(z)\rangle$.

We impose discrete Cauchy-Riemann (CR) on $\langle\psi_s(0)\psi_s(z)\rangle$:

$$\sum_{z\in\square}\langle\psi_s(0)\psi_s(z)\rangle\ \delta z = 0\,, \tag{B2}$$

where the sum is over the edges of an elementary plaquette of $\mathcal{L}^*$, and the δz's are the corresponding elementary displacements. For the discrete CR equations (B2) to hold, it is sufficient to fix the external loop configuration outside a given plaquette, and ask the total contribution of internal configurations to vanish[44,46]. This determines a linear system of equations for the Boltzmann weights. To get anisotropic solutions, we consider the analog problem on a rhombic lattice of angle α[45,46]. Setting

$$\lambda := e^{\frac{i\pi s}{2}}\,, \qquad \mu := e^{i\alpha(1+s)}\,, \tag{B3}$$

we get the 7×7 linear system for the unknowns $(t, u_1, u_2, v, w_1, w_2, x)$:

$$\begin{array}{rcl} t + \mu\lambda^{-2}u_1 - \mu u_2 - v &=& 0 \\ n^2u_1 - \lambda^{-2}u_2 - \mu\lambda^2 v + \mu\lambda^{-2}(n^2w_1 + w_2 + 2nx) &=& 0 \\ -\lambda^2 u_1 + n^2 u_2 + \mu\lambda^{-4}v - \mu(w_1 + n^2 w_2 + 2nx) &=& 0 \\ -\mu\lambda^2 u_1 + \mu\lambda^{-4}u_2 + n^2 v - \lambda^4 w_1 - \lambda^{-4}w_2 - 2x &=& 0 \\ n\lambda u_1 - n\lambda^{-1}u_2 - \mu\lambda^{-1}v + \mu\lambda^{-1}[n(w_1 + w_2) + (n^2+1)x] &=& 0 \\ n\lambda^{-1}u_1 - \lambda u_2 - n\mu\lambda v + \mu\lambda^{-3}(nw_1 + x) + \mu\lambda(w_2 + nx) &=& 0 \\ -u_1 + n\lambda^2 u_2 + n\mu\lambda^{-2}v - \mu\lambda^{-2}(w_1 + nx) - \mu\lambda^2(nw_2 + x) &=& 0\,, \end{array} \tag{B4}$$

As a first step, we need determine the spin s by going back to the isotropic case $\alpha = \pi/2$. Imposing $u_1 = u_2$ and $w_1 = w_2$, (B4) reduces to a 5×5 system, whose determinant is:

$$D(n, \lambda) = -\lambda^{-4}(\lambda^2 + 1)(n\lambda^4 - 1)^2(\lambda^4 + \lambda^{-4} + n^3 - 3n)\,. \tag{B5}$$

Using the parameterisation $n = -2\cos 2\theta$, this determinant vanishes when:

$$\exp(2i\pi s) = \exp(\pm 6i\theta)\,. \tag{B6}$$

For a general angle α, the solution of (B4) is a set of α-dependent weights $t(\alpha), \ldots x(\alpha)$. If we apply the substitution:

$$\alpha \to \frac{\varphi}{1+s}\,, \tag{B7}$$

we observe that the solution of (B4) is identical to the integrable weights (44). This is analogous to what was found for various other integrable models with a discrete holomorphic parafermion[44–46]. Note that the relation (B7) is consistent with the discussion on the Fermi velocity in Section III C.

Moreover, at the Ising points $\theta = \frac{\pi}{6}, \frac{5\pi}{6}$ (see Appendix C), the spin $s = \frac{1}{2}$ is consistent with (B6).

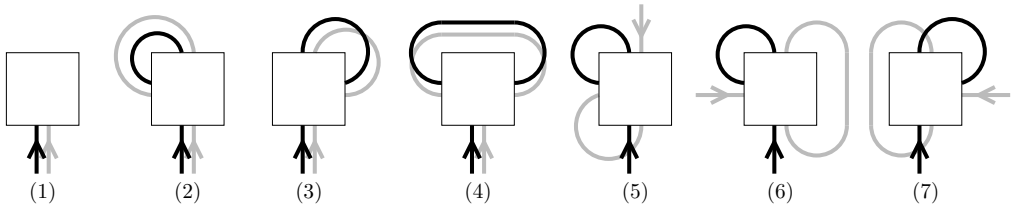

FIG. 16. External loop connectivities outside an elementary plaquette.

Appendix C: Free fermions at $\theta = \frac{\pi}{6}, \frac{5\pi}{6}$

1. Mapping to a staggered 8V model

At $\theta = \frac{\pi}{6}$ and $\theta = \frac{5\pi}{6}$, the model maps to a free fermion Hamiltonian through the mapping sequence:

$$\text{two-color loop} \to \text{square-lattice O}(n=1) \to \text{staggered 8V} \to \text{free fermions.}$$

In both cases, we start from the two-color loop model and do the sign change $(n, x) \to (-n, -x)$ to get $n = 1$. With this value of n, one may discard loop connectivities, and the model is simply local, with occupied and empty edges. After the exchange of occupied/empty edges, we get a square-lattice O(n) model[36] with $n = 1$ and weights :

$$\widetilde{t} = w_1 + w_2 - 2x, \quad \widetilde{u}_1 = u_1, \quad \widetilde{u}_2 = u_2, \quad \widetilde{v} = v, \quad \widetilde{w}_1 + \widetilde{w}_2 = t\,. \tag{C1}$$

(The tilde is here to avoid confusion between the O(n) and two-colour loop model Boltzmann weights). For $\theta = \frac{\pi}{6}$, we have the specific values

$$\begin{array}{rcl} \widetilde{t} &=& \sin 2\varphi - \sqrt{3} \\ \widetilde{u}_1 &=& \sqrt{3}\,\cos\varphi \\ \widetilde{u}_2 &=& -\sqrt{3}\,\sin\varphi \\ \widetilde{v} &=& \sin 2\varphi \\ \widetilde{w}_1 &=& -\cos(\tfrac{\pi}{6} - 2\varphi) - \tfrac{\sqrt{3}}{2} \\ \widetilde{w}_2 &=& \cos(\tfrac{\pi}{6} + 2\varphi) - \tfrac{\sqrt{3}}{2}\,, \end{array} \tag{C2}$$

which are exactly those of the integrable square-lattice O(n) model[36] with $n = 1$ at the dilute critical point. The O($n = 1$) model maps in turn to an eight-vertex model (see Fig. 17) with staggered weights

$$\begin{array}{rcl} \omega_1 = \omega_2 & = & \sqrt{3}\cos\varphi \\ \omega_3 = \omega_4 & = & -\sqrt{3}\sin\varphi \\ (\omega_5, \omega_6) & = & \begin{cases} (-\sin 2\varphi - \sqrt{3}, & \sin 2\varphi - \sqrt{3}) \quad \text{on even sites} \\ (\ \sin 2\varphi - \sqrt{3}, & -\sin 2\varphi - \sqrt{3}) \quad \text{on odd sites} \end{cases} \\ \omega_7 = \omega_8 & = & \sin 2\varphi\,. \end{array} \tag{C3}$$

At $\theta = \frac{5\pi}{6}$, one gets the same 8V model, up to irrelevant signs.

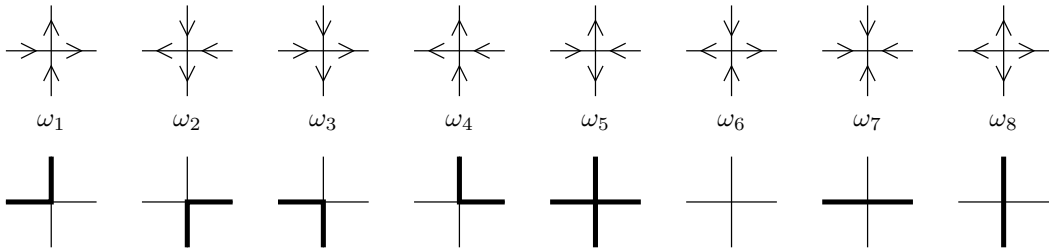

FIG. 17. Correspondence between the 8V model and the O($n = 1$) model. The mapping depicted here is valid on one sublattice, say even sites. On odd sites, all arrows must be reversed.

2. Very anisotropic limit: the XY chain in a magnetic field

In terms of the Pauli matrices σ_j, the 8V $\check{R}$-matrix reads:

$$\begin{aligned} \check{R}_j^{8\mathrm{V}} = & \frac{1}{4}(\omega_1 + \omega_2 + \omega_5 + \omega_6)\mathbf{1} + \frac{1}{4}(\omega_1 + \omega_2 - \omega_5 - \omega_6)\sigma_j^z\sigma_{j+1}^z \\ & + (\omega_3\ \sigma_j^-\sigma_{j+1}^+ + \omega_4\ \sigma_j^+\sigma_{j+1}^- + \omega_7\ \sigma_j^-\sigma_{j+1}^- + \omega_8\ \sigma_j^+\sigma_{j+1}^+) \\ & + \frac{1}{4}(\omega_1 - \omega_2)(\sigma_j^z + \sigma_{j+1}^z) + \frac{1}{4}(\omega_5 - \omega_6)(\sigma_j^z - \sigma_{j+1}^z)\,. \end{aligned} \tag{C4}$$

We can now take the very anisotropic limit $\varphi \to 0$. Denoting by a prime the derivative with respect to φ at $\varphi = 0$, and using the weights (C3), we obtain:

$$\check{R}_j'^{8\mathrm{V}} = -\sqrt{3}(\sigma_j^-\sigma_{j+1}^+ + \sigma_j^+\sigma_{j+1}^-) + 2(\sigma_j^-\sigma_{j+1}^- + \sigma_j^+\sigma_{j+1}^+) - (-1)^j(\sigma_j^z - \sigma_{j+1}^z)\,. \tag{C5}$$

The critical Hamiltonian is given by

$$H_0 = -\frac{1}{2}\sum_{j=1}^{L}\check{R}_j'^{8\mathrm{V}} = -\frac{1}{4}\sum_{j=1}^{L}\left[J_x\ \sigma_j^x\sigma_{j+1}^x - J_y\ \sigma_j^y\sigma_{j+1}^y + 2h\ (-1)^j\sigma_j^z\right]\,, \tag{C6}$$

where $J_x = (2 - \sqrt{3})$, $J_y = (2 + \sqrt{3})$ and $h = 2$. The alternating sign of the last term in (C6) can be eliminated by the unitary change of basis:

$$H_0 \to U^\dagger H_0 U\,, \qquad \text{where} \qquad U := \prod_{\ell=1}^{L/2}\sigma_{2\ell-1}^x\,. \tag{C7}$$

This maps H_0 to an XY chain in a magnetic field[47,48]:

$$H_{\mathrm{XY}} = U^\dagger H_0 U = -\frac{1}{2}\sum_{j=1}^{L}\left[(1+\gamma)\ \sigma_j^x\sigma_{j+1}^x + (1-\gamma)\ \sigma_j^y\sigma_{j+1}^y + h\ \sigma_j^z\right]\,, \tag{C8}$$

where $\gamma = -\frac{\sqrt{3}}{2}$ and $h = 2$. In particular, we have learnt that this particular point of the XY spin chain is exactly equivalent to the integrable dilute O($n = 1$) model.

3. Staggered perturbation associated to ν

The setting of the 8V model also allows us to consider a staggered perturbation like the one defining exponent ν (see Sec. V B). To do this, we introduce staggered spectral parameters $(1 \pm \lambda)\varphi$ on the even/odd sites. We take the very anisotropic limit $\varphi \to 0$, with λ fixed. This way, the parameter λ controls the strength of the perturbation. The resulting Hamiltonian has the form

$$H(\lambda) = H_0 + \lambda H_1$$

where

$$H_1 = -\frac{1}{2}\sum_{j=1}^{L}(-1)^j \check{R}_j'^{8\mathrm{V}} = -\frac{1}{4}\sum_{j=1}^{L}(-1)^j \ \left(J_x\ \sigma_j^x\sigma_{j+1}^x - J_y\ \sigma_j^y\sigma_{j+1}^y\right)\,, \tag{C9}$$

and J_x, J_y are the same as for H_0. After the unitary change of basis defined by U, we get the perturbing term:

$$H_p = U^\dagger H_1 U = -\frac{\lambda}{2}\sum_{j=1}^{L}(-1)^j \left[(1+\gamma)\ \sigma_j^x\sigma_{j+1}^x + (1-\gamma)\ \sigma_j^y\sigma_{j+1}^y\right]\,. \tag{C10}$$

Staggered 6V and 8V models were studied by various authors[49], but to our best knowledge, the case of the perturbation (C10) has not been treated. We will thus use the technique of[47] to solve it exactly.

4. Exact free-fermion solution

In this paragraph, we expose the exact solution of $H(\lambda)$ for general values of γ, h, λ. Following[47], we can solve the model $H(\lambda)$ by a Jordan-Wigner transformation, mapping the Pauli matrices σ_j to fermion operators

$$c_j := \left(\prod_{\ell=1}^{j-1}\sigma_\ell^z\right)\ \sigma_j^+\,, \qquad c_j^\dagger := \left(\prod_{\ell=1}^{j-1}\sigma_\ell^z\right)\ \sigma_j^-\,, \qquad c_j^\dagger c_j = \frac{1}{2}(1-\sigma_j^z)\,, \tag{C11}$$

obeying anti-commutation relations:

$$\{c_j, c_\ell\} = 0\,, \qquad \{c_j, c_\ell^\dagger\} = \delta_{j\ell}\,. \tag{C12}$$

In this language, the perturbed Hamiltonian reads

$$H(\lambda) = -\sum_{j=1}^{L}\left\{\left[1+(-1)^j\lambda\right]\left[c_j^\dagger c_{j+1} + c_{j+1}^\dagger c_j + \gamma(c_j^\dagger c_{j+1}^\dagger + c_{j+1}c_j)\right] + h\left(\frac{1}{2} - c_j^\dagger c_j\right)\right\}. \tag{C13}$$

We introduce two species of fermions

$$c_{1,\ell} := c_{2\ell}\,, \qquad c_{2,\ell} := c_{2\ell-1}\,, \tag{C14}$$

and their Fourier modes

$$c_{\mu,q} := \frac{1}{\sqrt{L/2}}\sum_{\ell=1}^{L/2} e^{i\ell q}c_{\mu,\ell}\,, \qquad q = \frac{2\pi m}{L/2} - \pi\,, \quad m = 1,\dots,\frac{L}{2}\,. \tag{C15}$$

We can now rewrite $H(\lambda)$ as

$$H(\lambda) = \sum_{-\pi<q\le\pi}\sum_{\mu,\nu}\left[c_{\mu,q}^\dagger A_{\mu\nu,q}c_{\nu,q} + \frac{1}{2}\left(c_{\mu,q}^\dagger B_{\mu\nu,q}c_{\nu,-q}^\dagger - c_{\mu,-q}B_{\mu\nu,q}c_{\nu,q}\right)\right]\,, \tag{C16}$$

where the matrices A_q and B_q read

$$A_q = \begin{pmatrix} h & \alpha_q^* \\ \alpha_q & h\end{pmatrix}\,, \qquad B_q = \begin{pmatrix} 0 & -\beta_q^* \\ \beta_q & 0\end{pmatrix}\,, \qquad \begin{array}{rcl}\alpha_q &:=& -[(1+\lambda)e^{iq} + (1-\lambda)]\,,\\ \beta_q &:=& \gamma[(1+\lambda)e^{iq} - (1-\lambda)]\,.\end{array} \tag{C17}$$

Like in[47], the energies $\epsilon_\mu(q)$ are the square roots of the eigenvalues of $(A_q + B_q)(A_q - B_q)$:

$$\epsilon_{1,2}(q) = 2\sqrt{\frac{h^2}{4} + (1+\gamma^2\lambda^2)\cos^2\frac{q}{2} + (\gamma^2+\lambda^2)\sin^2\frac{q}{2} \mp \sqrt{4\gamma^2\lambda^2 + h^2\left|\cos\frac{q}{2} + i\lambda\sin^2\frac{q}{2}\right|^2}}. \tag{C18}$$

This is the two-branch dispersion relation for arbitrary γ, h, λ.

To express the corresponding eigenmodes, we need the unitary 2×2 matrices W_q, V_q defined by the linear relations

$$(A_q - B_q)W_q = V_q D_q\,, \qquad (A_q + B_q)V_q = W_q D_q\,, \qquad D_q := \begin{pmatrix} \epsilon_1(q) & 0 \\ 0 & \epsilon_2(q) \end{pmatrix}. \tag{C19}$$

The Bogoliubov transformation diagonalising $H(\lambda)$ is

$$\eta_{\mu,q} := \frac{1}{2}\sum_\nu \left[(W+V)^\dagger_{\mu\nu,q}\, c_{\nu,q} - (W-V)^\dagger_{\mu\nu,q}\, c^\dagger_{\nu,-q}\right]. \tag{C20}$$

Unitarity of V_q and W_q ensures the canonical anticommutation relations

$$\{\eta_{\mu,q}, \eta_{\mu',q'}\} = 0\,, \qquad \{\eta_{\mu,q}, \eta^\dagger_{\mu',q'}\} = \delta_{\mu\mu'}\delta_{qq'}\,. \tag{C21}$$

In terms of the η's, the Hamiltonian reads

$$H(\lambda) = \sum_{-\pi<q\le\pi}\ \sum_{\mu=1,2} \epsilon_\mu(q)\,\eta^\dagger_{\mu,q}\eta_{\mu,q}\,. \tag{C22}$$

Note that there are $L/2$ distinct momenta q, and that each momentum corresponds to two modes $\mu = 1, 2$. Thus, we recover L independent modes $\eta_{\mu,q}$.

As a final step, we perform the change

$$\eta_{\mu,q} \to \widetilde{\eta}_{\mu,q} = \begin{cases} \eta_{\mu,q} & \text{if } q \ge 0, \\ \eta^\dagger_{\mu,q} & \text{if } q < 0, \end{cases} \tag{C23}$$

so that the modes with $q < 0$ are now considered as holes. the Hamiltonian becomes

$$H(\lambda) = \sum_{-\pi<q\le\pi}\ \sum_{\mu=1,2} \widetilde{\epsilon}_\mu(q)\,\widetilde{\eta}^\dagger_{\mu,q}\widetilde{\eta}_{\mu,q}\,, \qquad \text{where} \qquad \widetilde{\epsilon}_\mu(q) := \mathrm{sgn}(q)\,\epsilon_\mu(q)\,. \tag{C24}$$

5. Critical Majorana fermion at $h = 2, \lambda = 0$

The dispersion relation of the XY chain in a magnetic field is obtained by setting $\lambda = 0$ in (C18):

$$\epsilon_{1,2}(q) = 2\sqrt{\left(\frac{h}{2} \mp \cos\frac{q}{2}\right)^2 + \gamma^2\sin^2\frac{q}{2}} \qquad (\lambda = 0)\,. \tag{C25}$$

For $h = 2$, ϵ_1 is critical at $q = 0$, whereas ϵ_2 is not critical[50]:

$$\widetilde{\epsilon}_1(q) = 4\sin\frac{q}{4}\sqrt{\sin^2\frac{q}{4} + \gamma^2\cos^2\frac{q}{4}} \tag{C26}$$

$$\widetilde{\epsilon}_2(q) = 4\,\mathrm{sgn}(q)\cos\frac{q}{4}\sqrt{\cos^2\frac{q}{4} + \gamma^2\sin^2\frac{q}{4}}\,. \tag{C27}$$

The dispersion relation $\widetilde{\epsilon}_1(q)$ is approximately linear at $q = 0$ (see Fig. 18). In the ground state, all levels with $-\pi < q < 0$ are filled: this is a Fermi sea with only one Fermi level $q_f = 0$, and thus it corresponds to a Majorana fermion with central charge $c = \frac{1}{2}$. The critical eigenmodes are obtained from (C20):

$$\begin{cases} \eta_{1,q} &= \cos\frac{\theta_{1,q}}{2}\,(c_{1,q} + c_{2,q}) + i\sin\frac{\theta_{1,q}}{2}\,(c^\dagger_{1,-q} + c^\dagger_{2,-q})\,, \\ \eta_{2,q} &= \cos\frac{\theta_{2,q}}{2}\,(c_{1,q} - c_{2,q}) + i\sin\frac{\theta_{2,q}}{2}\,(c^\dagger_{1,-q} - c^\dagger_{2,-q})\,, \end{cases} \tag{C28}$$

where

$$\begin{cases} \theta_{1,q} &:= \text{Arg}\left(1-\cos\frac{q}{2}-i\sin\frac{q}{2}\right), \\ \theta_{2,q} &:= \text{Arg}\left(1+\cos\frac{q}{2}+i\sin\frac{q}{2}\right). \end{cases} \tag{C29}$$

After the change $\eta \to \widetilde{\eta}$ (C23), the continuum limit is described by the effective Hamiltonian

$$H_0 \simeq iv_f \int \mathrm{d}x\ \widetilde{\eta}_1^\dagger \partial_x \widetilde{\eta}_1\,. \tag{C30}$$

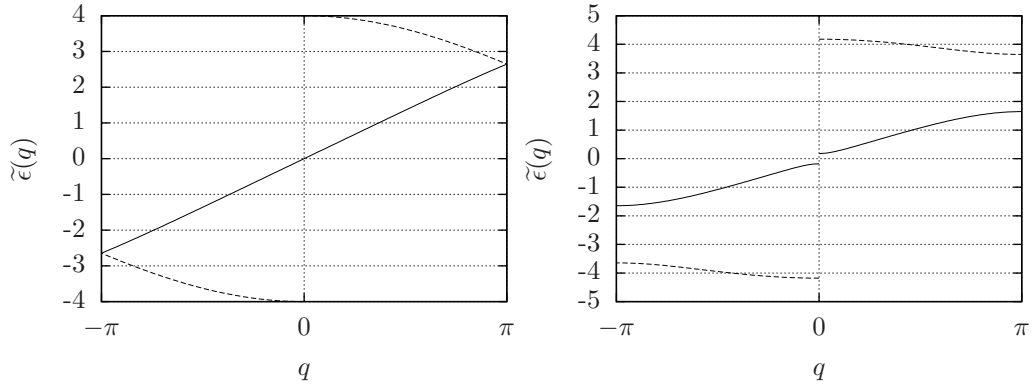

FIG. 18. The dispersion relation for $h = 2, \gamma = -\frac{\sqrt{3}}{2}$. Left: critical case $\lambda = 0$. Right: $\lambda = \frac{1}{2}$. The full (resp. dotted) lines represent $\widetilde{\epsilon}_1$ (resp. $\widetilde{\epsilon}_2$).

6. Gapped theory at $h = 2, \lambda > 0$

When the λ perturbation is turned on, an energy gap opens at $q = 0$ (see Fig. 18):

$$\Delta E := 2\epsilon_1(q=0) = 2\left|\sqrt{1+\gamma^2\lambda^2}-1\right| \sim \gamma^2\lambda^\nu\,, \qquad \nu = 2\,. \tag{C31}$$

To understand this value of ν, we shall analyse the perturbing term H_p in terms of the critical modes $\widetilde{\eta}_{1,q}$ (C28). The relations (C28) can be inversed, to give:

$$\begin{cases} c_{1,q}+c_{2,q} &= \cos\frac{\theta_{1,q}}{2}\,\eta_{1,q} - i\sin\frac{\theta_{1,q}}{2}\,\eta_{1,-q}^\dagger := a_{1,q}\,, \\ c_{1,q}-c_{2,q} &= \cos\frac{\theta_{2,q}}{2}\,\eta_{2,q} - i\sin\frac{\theta_{2,q}}{2}\,\eta_{2,-q}^\dagger := a_{2,q}\,. \end{cases} \tag{C32}$$

The perturbing term has the expression

$$\begin{aligned} H_p = \frac{1}{2}\sum_{-\pi<q\le\pi} \Big\{ & (1-\cos q)\,(a_{1,q}^\dagger a_{1,q} - a_{2,q}^\dagger a_{2,q}) \\ & + i\sin q\,\left[a_{2,q}^\dagger a_{1,q} + \frac{\gamma}{2}\,(a_{1,q}^\dagger a_{1,-q}^\dagger - a_{2,q}^\dagger a_{2,-q}^\dagger) - \text{h.c.}\right] \\ & - \gamma(1+\cos q)\,(a_{2,q}^\dagger a_{1,-q}^\dagger + a_{1,-q}a_{2,q}) \quad \Big\}. \end{aligned} \tag{C33}$$

In the region $q \simeq 0$, the first term in (C33) is of order q^2, and thus it generates irrelevant terms of the form $\widetilde{\eta}_1^\dagger \partial_x^2 \widetilde{\eta}_1$ in the continuum limit. The second term is of order q, and corresponds to $\widetilde{\eta}_1^\dagger \partial_x \widetilde{\eta}_1$, which renormalises the Fermi velocity. At first order in λ, the third term has no effect on the continuum theory. However, in second-order perturbation in λ, it generates terms of the form $(\widetilde{\eta}_2^\dagger \widetilde{\eta}_2)(\widetilde{\eta}_1^\dagger \widetilde{\eta}_1)$, which are non-vanishing since the lowest $\widetilde{\eta}_2$ modes are occupied in the ground state. From this analysis, we obtain the effective Hamiltonian in the continuum limit

$$H_{\text{eff}}(\lambda) \propto \int \mathrm{d}x\ \left(i\,\widetilde{\eta}_1^\dagger \partial_x \widetilde{\eta}_1 + \text{const}\times\gamma^2\lambda^2\,\widetilde{\eta}_1^\dagger \widetilde{\eta}_1\right). \tag{C34}$$

The "mass term" has dimension $X_t = 1$, and the energy gap thus scales as

$$\Delta E \propto \left(\lambda^2\right)^{\frac{1}{2-X_t}} \ .$$

Comparing with (C31), we get the scaling relation

$$X_t = 2 - \frac{2}{\nu} \, . \tag{C35}$$

[1] H. Levine, S. B. Libby and A. M. M. Pruisken, Phys. Rev. Lett. **51**, 1915 (1983)
[2] A. M. M. Pruisken, in *The Quantum Hall Effect*, ed. R. E. Prange and S. M. Girvin (Springer-Verlag, New York, 1990)
[3] H. P. Wei, D. C. Tsui, M. A. Paalanen and A. M. M. Pruisken, Phys. Rev. Lett. **61**, 1294 (1988)
[4] J. T. Chalker and P. D. Coddington, J. Phys. **C 21**, 2665 (1988)
[5] B. Huckestein, Rev. Mod. Phys. **67**, 357 (1995) [cond-mat/9501106]
[6] P. Cain, R. A. Romer and M. E. Raikh, Phys. Rev. **B 67**, 075307 (2003)
[7] K. Slevin and T. Ohtsuki, Phys. Rev. **B 80**, 041304 (2009) [0905.1163]
[8] G. V. Mil'nikov and I. M. Sokolov, JETP Lett. **48**, 536 (1988)
[9] A. W. W. Ludwig, M. P. A. Fisher, R. Shankar and G. Grinstein, Phys. Rev. **B 50**, 7526 (1994)
[10] J. Kondev and J. B. Marston, Nucl. Phys. **B 497**, 63 (1997)
[11] J. B. Marston and S.-W. Tsai, Phys. Rev. Lett. **82**, 4906 (1999)
[12] A. Sedrakyan, Nucl. Phys. **B 554** 514 (1999);
A. Sedrakyan, Proceedings of Advanced NATO Workshop on Statistical Field Theories, Como, June 18-23 (2001);
A. Sedrakyan, Phys. Rev. **B 68**, 235329 (2003)
[13] V. Kagalovsky, B. Horovitz, Y. Avishai and J. T. Chalker, Phys. Rev. Lett. **82**, 3516 (1999)
[14] H. Saleur and B. Duplantier, Phys. Rev. Lett. **58**, 2325 (1987)
[15] I. A. Gruzberg, A. W. W. Ludwig and N. Read, Phys. Rev. Lett. **82**, 4524 (1999)
[16] E. J. Beamond, J. Cardy and J. T. Chalker, Phys. Rev. **B 65**, 214301 (2002)
[17] J. Cardy, Commun. Math. Phys. **258**, 87 (2005)
[18] S. O. Warnaar and B. Nienhuis, J. Phys. A: Math. Gen. **26**, 2301 (1993)
[19] M. J. Martins and B. Nienhuis, J. Phys. A: Math. Gen. **31**, L723 (1998)
[20] P. Fendley and J. L. Jacobsen, J. Phys. A: Math. Gen. **41**, 215001 (2008)
[21] J. Birman and H. Wenzl, Trans. Am. Math. Soc. **313**, 249 (1989);
J. Murakami, Osaka J. Math. **24**, 745 (1987)
[22] H. Au-Yang and J. H. H. Perk, Intern. J. Mod. Phys. **A**, Vol. 7, Suppl. 1B 1025 (1992)
[23] K. Efetov, *Supersymmetry in Disorder and Chaos* (Cambridge University Press, 1999)
[24] B. Nienhuis, Phys. Rev. Lett. **49**, 1062 (1982)
[25] M. Janssen, M. Metzler and M. R. Zirnbauer, Phys. Rev. **B 59**, 15836 (1999)
[26] E. Bettelheim, I. A. Gruzberg and A. W. W. Ludwig, private communication
[27] B. Duplantier and H. Saleur, Nucl. Phys. **B 290**, 291 (1987)
[28] U. Grimm, Lett. Math. Phys. **32**, 183 (1994);
U. Grimm and S. O. Warnaar, Nucl. Phys. **B 435**, 482 (1995)
[29] C. M. Fortuin and P. W. Kasteleyn, Physica **57**, 536 (1972)
[30] H. Temperley and E. H. Lieb, Proc. Roy. Soc. (London) **A322**, 251 (1971)
[31] M. Wadati, T. Deguchi and Y. Akustu, Phys. Rep. **180**, 247 (1989)
[32] H. W. J. Blöte, J. L. Cardy and M. P. Nightingale, Phys. Rev. Lett. **56**, 742 (1986);
I. Affleck, Phys. Rev. Lett. **56**, 746 (1986)
[33] R. J. Baxter, *Exactly Solved Models in Statistical Mechanics* (Academic, London, 1982).
[34] S. O. Warnaar, P. A. Pearce, K. A. Seaton and B. Nienhuis, J. Stat. Phys. **74**, 469 (1994)
[35] Ph. Di Francesco, P. Mathieu and D. Sénéchal, *Conformal Field Theory* (Springer, New York, 1997) and references therein
[36] H. W. J. Blöte and B. Nienhuis, J. Phys. A: Math. Gen. **22**, 1415 (1989)
[37] I. Vaysburd, Nucl. Phys. **B 446**, 387 (1995)
[38] P. Fendley, J. Phys. A: Math. Gen. **39**, 15445 (2006)
[39] E. Date, M. Jimbo, T. Miwa and M. Okado, Lett. Math. Phys. **12**, 209 (1986) [Erratum-ibid. **14**, 97 (1987)]
[40] A. B. Zamolodchikov, Nucl. Phys. **B 366**, 122 (1991)
[41] A. B. Zamolodchikov, Mod. Phys. Lett. **6**, 1807 (1991)
[42] Y. Ikhlef, J. L. Jacobsen and H. Saleur, J. Phys. **A 43**, 225201 (2010)
[43] Q. Liu, Y. Deng and T. M. Garoni, Nucl. Phys. **B 846**, 283 (2011)
[44] V. Riva and J. Cardy, J. Stat. Mech. P12001 (2007)
[45] M. A. Rajabpour and J. Cardy, J. Phys. A: Math. Gen. **40**, 14703 (2007)
[46] Y. Ikhlef and J. Cardy, J. Phys. A: Math. Gen. **42**, 102001 (2009)
[47] E. Lieb, T. Schultz and D. Mattis, Ann. Phys. **16**, 407 (1961)
[48] T. D. Schultz, D. C. Mattis and E. H. Lieb, Rev. Mod. Phys. **36**, 856 (1964)
[49] J. H. H. Perk, H. W. Capel, M. J. Zuilhof and Th. J. Siskens, Physica **A 81**, 319 (1975);
F. Y. Wu and K. Y. Lin, Phys. Rev. **B 12**, 419 (1975);
C. S. Hsue, K. Y. Lin and F. Y. Wu, Phys. Rev. **B 12**, 429 (1975)
[50] In the case $h = \gamma = 0$, both modes ϵ_1, ϵ_2 are critical at $q = \pi$, and the corresponding field theory is a critical Dirac fermion.